OFFICE OF NAVAL RESEARCH

Grant N00014-90-J-1193

TECHNICAL REPORT No. 80

Rare Gas Clusters Containing Charged Atoms

by

Isidore Last and Thomas F. George

Prepared for publication

in

Current Topics in Ion Chemistry and Physics, Volume 1
Edited by C. Y. Ng, T. Baer and I. Powis (Wiley, New York, 1992)

Departments of Chemistry and Physics
Washington State University
Pullman, WA 99164-1046

March 1992

UNCLASSIFIED
SECURITY CLASSIFICATION OF THIS PAGE

REPORT DOCUMENTATION PAGE

Form Approved
OMB No. 0704-0188

1a. REPORT SECURITY CLASSIFICATION Unclassified	1b. RESTRICTIVE MARKINGS
2a. SECURITY CLASSIFICATION AUTHORITY	3. DISTRIBUTION/AVAILABILITY OF REPORT Approved for public release; distribution unlimited
2b. DECLASSIFICATION/DOWNGRADING SCHEDULE	
4. PERFORMING ORGANIZATION REPORT NUMBER(S) WSU/DC/92/TR-80	5. MONITORING ORGANIZATION REPORT NUMBER(S)
6a. NAME OF PERFORMING ORGANIZATION Depts. Chemistry & Physics Washington State University 6b. OFFICE SYMBOL (If applicable)	7a. NAME OF MONITORING ORGANIZATION
6c. ADDRESS (City, State, and ZIP Code) 428 French Administration Building Pullman, WA 99164-1046	7b. ADDRESS (City, State, and ZIP Code) Chemistry Program 800 N. Quincy Street Arlington, Virginia 22217
8a. NAME OF FUNDING/SPONSORING ORGANIZATION Office of Naval Research 8b. OFFICE SYMBOL (If applicable)	9. PROCUREMENT INSTRUMENT IDENTIFICATION NUMBER Grant N00014-90-J-1193
8c. ADDRESS (City, State, and ZIP Code) Chemistry Program 800 N. Quincy Street Arlington, Virginia 22217	10. SOURCE OF FUNDING NUMBERS PROGRAM ELEMENT NO. / PROJECT NO. / TASK NO / WORK UNIT ACCESSION NO.

11. TITLE (Include Security Classification)
Rare Gas Clusters Containing Charged Atoms

12. PERSONAL AUTHOR(S)
Isidore Last and Thomas F. George

13a. TYPE OF REPORT	13b. TIME COVERED	14. DATE OF REPORT (Year, Month, Day)	15. PAGE COUNT
	FROM _____ TO _____	March 1992	57

16. SUPPLEMENTARY NOTATION
Prepared for publication in Current Topics in Ion Chemistry and Physics, Volume 1
Edited by C. Y. Ng, T. Baer and I. Powis (Wiley, New York, 1992)

17. COSATI CODES		
FIELD	GROUP	SUB-GROUP

18. SUBJECT TERMS (Continue on reverse if necessary and identify by block number)
RARE GAS CLUSTERS
CONTAINING CHARGED ATOMS
HALOGEN ATOMS
SEMIEMPIRICAL METHODS
DIATOMICS-IN-IONIC-SYSTEMS
COMPARE WITH EXPERIMENTS

19. ABSTRACT (Continue on reverse if necessary and identify by block number)

Three kinds of rare gas (R) containing clusters are considered in this article: (I) ionic clusters R_n^+ and $(R_nM)^+$, M being another atom or a molecule, (II) neutral rare gas-halogen clusters R_nX with $R \rightarrow X$ electron transfer, and (III) Rydberg excited R_n^* clusters. These clusters have much in common, as all of them contain ions or ionic cores, with the positive charge delocalized mostly between some number of atoms. Such systems can be treated by the semiempirical diatomics-in-ionic-systems (DIIS) method. We present in this article a brief description of the DIIS method and the results of its applications to the kinds of clusters mentioned above. The article presents also discussions of results obtained by other theoretical methods and experimental studies.

20. DISTRIBUTION/AVAILABILITY OF ABSTRACT	21. ABSTRACT SECURITY CLASSIFICATION
☒ UNCLASSIFIED/UNLIMITED ☒ SAME AS RPT ☐ DTIC USERS	Unclassified
22a. NAME OF RESPONSIBLE INDIVIDUAL Dr. John C. Pazik	22b. TELEPHONE (Include Area Code) (202) 696-4410 / 22c. OFFICE SYMBOL

DD Form 1473, JUN 86 *Previous editions are obsolete.*

SECURITY CLASSIFICATION OF THIS PAGE
UNCLASSIFIED

To appear in *Current Topics in Ion Chemistry and Physics*, Volume 1
Edited by C. Y. Ng, T. Baer and I. Powis (Wiley, New York, 1992)

RARE GAS CLUSTERS CONTAINING CHARGED ATOMS

Isidore Last

Department of Physics and Applied Mathematics

Soreq Nuclear Research Center

Yavne 70600, ISRAEL

Thomas F. George

Departments of Chemistry and Physics

Washington State University

Pullman, Washington 99164-1046, USA

Abstract

Three kinds of rare gas (R) containing clusters are considered in this article: (I) ionic clusters R_n^+ and $(R_nM)^+$, M being another atom or a molecule, (II) neutral rare gas-halogen clusters R_nX with $R \rightarrow X$ electron transfer, and (III) Rydberg excited R_n^* clusters. These clusters have much in common, as all of them contain ions or ionic cores, with the positive charge delocalized mostly between some number of atoms. Such systems can be treated by the semiempirical diatomics-in-ionic-systems (DIIS) method. We present in this article a brief description of the DIIS method and the results of its applications to the kinds of clusters mentioned above. The article presents also discussions of results obtained by other theoretical methods and experimental studies.

I. Introduction

The interaction between neutral ground-state rare gas atoms is of a simple nature since they (i) have closed-shell electronic structure and are unable to form chemical bonds, (ii) are spherically symmetrical, and (iii) can be excited to Rydberg states only. Due to these features, the structure of the molecules, clusters, liquids and solids formed by rare gas atoms is determined mainly by the atomic sizes and the interatomic attractive van der Waals (vdW) forces.[1-6] The interaction becomes more complicated when other kinds of atoms or molecules are involved, but except for some very special cases, this interaction does not significantly effect the electronic structure of the rare gas atoms.[7-9] The features of a rare gas atom are changed dramatically if an electron is removed from a closed shell as the result of atomic ionization or excitation. The rare gas atom with an electron deficiency in the outer shell is chemically active and is then able to form strongly-bound molecules and clusters whose structure is more intricate than that of the vdW clusters.[10-16] In the case of a deficiency on an inner shell, the atom is unstable, which leads to photon emission or autoionization.

We can distinguish three kinds of systems formed by rare gas atoms with electron deficiency: (i) molecular and cluster ions, (ii) molecules, clusters and solids with Rydberg-excited rare gas atoms, (iii) molecules, clusters and solids with electron transfer from a rare gas atom to another kind of atom--halogen atom, mostly. All these systems have much in common, as their properties are determined to a great degree by the properties of the rare gas ionic cores which are the same in the ionic and excited states. The theoretical consideration of these systems is relatively complex, first of all because of the presence of charged particles and their interaction with the neutral atoms which they have polarized. Further complication arises because of the electrostatic interaction of the polarized atoms with one another. Dealing with the systems with the electron deficiency, we also have to take into account the delocalization of the electron deficiency between rare gas atoms. Because of this delocalization, one needs to take a quantum chemistry approach in order to consider such systems. Experimental spectroscopic

studies of ionized and excited molecules and clusters containing rare gas atoms have much in common, but with one important difference: namely that only the ionic species can be tested by mass spectroscopy, so that the masses of the neutral, both ground state and excited, clusters cannot be determined directly.[17]

Considering the ionized or excited clusters, we have to distinguish between two different problems. The first is the study of the geometry and spectroscopy of stable ionic or metastable excited clusters. Another problem is the study of ionization potentials and excitation energies of neutral ground-state clusters. It is important to note that the formation of ionic clusters involves often as an intermediate stage the Rydberg excitations whose study is necessary to understand better the ionization dynamics. However, the dynamical problems of the formation and decay of ionic and excited clusters will be not considered at length in this review article.

Without going into the semantic discussion of the term "cluster" (there are some differences on this point in the literature), we shall use this term here to refer to rare gas containing systems with more than two atoms whose dissociation or atomic detachment energy is small, less than, say 0.5 eV. The name "cluster" shall apply not only to stable or metastable systems but also to unstable systems formed as a result of cluster ionization or excitation. Any stable or metastable diatomic, even that weakly bound, shall be called by the name "molecule."

In the next section we shall discuss briefly the chemical properties of rare gas atoms and the structure of neutral vdW clusters. In Section III we will discuss the calculation of the polarization energy. In Section IV we will review the semiempirical method called diatomics-in-ionic systems (DIIS) which we have developed for the study of rare gas systems with charged atoms. Ionic clusters will be considered in Sections V and VI. Excited clusters with electron transfer and Rydberg-excited clusters will be considered in Sections VII and VIII, respectively. Concluding remarks are given in Section IX.

II. Chemical Properties of Neutral Ground State Rare Gas Atoms

In their neutral ground state, rare gas atoms have a closed-shell structure with the $(np)^6$ outer shell. Because of such structure they are chemically-inert atoms, at least as they interact with other closed-shell atoms or molecules. Being chemically inert, rare gas atoms interact by vdW forces only, which at large distances are represented by attractive dispersion forces roughly proportional to the polarizabilities of the interacting species. At small distances the dispersion forces are overcome by strong repulsive forces which determine the atomic vdW radius. The rare gas atoms vdW radii and polarizabilities, as well as the ionization potentials, are presented in Table 1. In the lowest ionized state, the outer shell structure becomes $(np)^5$, with an electron deficiency on a np orbital. This electronic structure, similar to that of halogen atoms, makes the rare gas ions chemically active. The diatomic molecules formed by rare gas ions, such as R_2^+ [10,18-20] and $(RX)^+$ [21-27], are chemically stable molecules whose dissociation energy exceeds mostly 1 eV.

The geometrical structures of the weakly-bound vdW molecules R_2 or RR' and clusters R_n are determined by the vdW radii of their component atoms.[1,5,28,29] The experimental equilibrium distances and the dissociation energies of the rare gas diatomic molecules[29] are presented in Table 2. The equilibrium geometry of the rare gas vdW clusters can be described as the most compact packing of almost rigid spheres.[30] For example, three rare gas atoms form an equilateral triangle and four rare gas atoms form an equilateral pyramid. The first most stable R_n cluster with magic number n=13 is formed by a central atom and 12 atoms symmetrically located around the central one. The next "magic" cluster R_{55} has two closed coordinate spheres (1+12+42).[30] Because of the pairwise character of the vdW forces and their short radii, the cluster energy is practically equal to the sum of the interaction energies between all neighbor pairs. The mutual attraction between several atoms in vdW clusters leads to some small decrease in the equilibrium interatomic distances compared to those of diatomic vdW molecules, which is demonstrated for Ar_n clusters in Table 3, where the dissociation and atom detachment

energies of these clusters are presented as well. It is important, however, to note that due to thermal motion in the weakly-bound vdW clusters, the atoms are mostly localized far away from the equilibrium (minimum energy) positions. Rare gas atoms form typical vdW clusters also with nonpolar molecules, such as halogen X_2 molecules[31-33] or aromatic molecules.[34-35] Somewhat more complicated and more strongly-bound clusters are formed by rare gas atoms with polar molecules which contribute to attractive polarization forces in addition to usual vdW forces.[36-39] All these clusters have much in common, as the electronic structures of the component atoms and molecules are unaffected by one another (except for polarization in the presence of polar molecules). The mutual independence of atomic and molecular electronic structures in vdW clusters is well demonstrated by the weak effect of the constituent rare gas atoms on the valence spectrum of a molecular cluster.[40-42] Since the electrons in the vdW clusters are strongly localized, the cluster wave function can be presented as the antisymmetrized product of atomic and molecular wave functions

$$\Phi = \hat{A} \prod_{j=1} \chi_j \quad , \tag{II.1}$$

where χ_j are the group functions describing individual atoms and molecules.[43]

The electronic structure of rare gas atoms can be affected by open-shell radicals with high electron affinity, particularly by halogen atoms X. Due to the high electron affinity of halogen atoms, the excitation energy of the states with electron transfer (R^+X^-) is relatively low, for example 4 eV in XeCl molecule.[44] Taking into account the coupling between the nonpolar (RX) and polar (R^+X^-) electronic structures, the RX wave function has to be described as the supperposition

$$\Phi = C_1\Phi_{RX} + C_2\Phi_{R^+X^-} \quad . \tag{II.2}$$

Because of the coupling between these two electronic structures, the ground-state R_nX systems cannot be considered as pure vdW complexes, since the coupling contributes to some valence attraction between the halogen and rare

gas atoms.[45] For example, the contribution of the coupling (valence) energy constitute 45% of the XeCl dissociation energy, and the Xe-Cl equilibrium distance (3.23Å) is much smaller than the sum of the vdW radii of Xe and Cl atoms (4Å).[8] The coupling between the nonpolar and polar (ionic) configurations becomes much more important in the case of the heavy rare gas atoms Xe and Kr and light halogen atom F, leading, e.g., to the formation of XeF_3 and XeF_4 molecules.[46-48]

III. Polarization Energy and Charge Motion Effects

The presence of charged particles, such as R^+ ions in ionic R_n^+ clusters, ionic cores and electrons in Rydberg excited clusters, and R^+ and X^- ions in excited clusters with electron transfer, results in the polarization of neutral atoms and molecules. When the charges in a cluster are strongly localized on some atoms, the polarization energy can be easily represented in the point-dipole approximation[49] by

$$P = P^{(1)} + P^{(2)} \tag{III.1}$$

$$P^{(1)} = -\sum_j A_j \left(\sum_i q_i Z_{ij}\right)^2 \tag{III.2}$$

$$P^{(2)} = e^2 \sum_j \alpha_j \sum_{j'} \alpha_{j'} \sum_{mn} \Gamma_{jj',mn} \sum_i^I q_i Z_{ij,m} Z_{ij',n} \quad , \qquad j'>j \tag{III.3}$$

where q_i are the ion charges in the electron e units, α_j are the neutral atoms polarizabilities (Table 1), and A_j are the parameters which determine the atomic polarization energy,

$$A_j = \alpha_j e^2/2 \quad . \tag{III.4}$$

Z_{ij} are the vectors proportional to the electrostatic field,

$$Z_{ij} = (R_i - R_j)/R_{ij}^3 \quad . \tag{III.5}$$

R_i and R_j being the radius vectors of charged and neutral atoms, respectively, and $\Gamma_{jj',mn}$ are the tensors of dipole-dipole interaction,

$$\Gamma_{jj'mn} = 3(R_j - R_{j'})_m(R_j - R_{j'})_n/R^5_{jj'} - \delta_{mn}/R^3_{jj'} \qquad \text{(III.6)}$$

where m,n = 1,2,3 denote the x,y,z projections and δ_{mn} is the Kronecker delta. The number of charged particles (ions) is I = 1 in ionic clusters and I = 2 (X^- and R^+) in clusters with electron transfer from R to X. The first term, $P^{(1)}$, in Eq. (III.1) gives the energy of the interaction between the charged particles (i = 1...I) and the neutral atoms which they polarize, whereas the second term, $P^{(2)}$, gives the energy of the dipole-dipole interaction between the polarized atoms. The contribution of the dipole-dipole interaction is supposed to be small compared with the direct charge-neutral atoms interaction.

The polarization energy presents some difficulties in the theoretical consideration of clusters with charged atoms. First, the polarization energy is not of pairwise character, except for the case of one charge and the neglect of the second (dipole-dipole) term in Eq. (III.1). Second, using the electrostatic expressions in the point-dipole approximation, we are neglecting the overlap of the ion and the atom which it polarizes, leading to the unphysical divergence of the interaction energy at small separations. Third, the ionic charge is often delocalized between two or more atoms. The first of these problems will be considered in the next section within the framework of the DIIS method. The unphysical behavior of the ion-atom polarization energy (III.2) at small separations is usually avoided by introducing a damping function γ into the polarization energy expression,[50]

$$P_{iA} = -A_A \frac{\gamma(R)}{R^4} \quad , \qquad \text{(III.7)}$$

where R is the separation between the ion i and atom A. Different damping function expressions have been proposed for the ion-atom[14,50-53] and electron-atom[54-56] interactions. If the correct asymptotic conditions are satisfied, the form of the dependence of γ on R does not imply much about the results.

For example, according to our estimates, different reasonable models for the damping function $\gamma(R)$ result in variations of the energy of Ar_n^+ clusters within a range of only 0.003 eV. We have suggested[14] to take the damping function in the form

$$\gamma(R) = \left[1 + \left(\frac{\rho_i+\rho_A}{R}\right)^{12}\right]^{-1/3} , \qquad \text{(III.8)}$$

where ρ_i and ρ_A are the atomic radii of the ion and atom, respectively. For the values ρ_i and ρ_A in the Eq. (III.8), we are using the atomic vdW radii. When the interatomic separation R is larger than the sum of atomic radii (non-overlapping atoms), the function γ is close to unity, i.e., the point-dipole approximation is valid. When the interatomic separation is smaller than the sum of atomic radii (overlapping atoms), the damping function decreases as R^{-4}, so that the ion-atom polarization energy (III.7) is saturated with a limiting value of $-C_A/(\rho_i+\rho_A)^4$. Introducing the damping function (III.8) into Eqs. (III. 2-3), we obtain the following expression for the polarization energy of a polyatomic system:

$$P^{(1)} = -\sum_j A_j \left(\sum_i^I q_i \sqrt{\gamma_{ij}}\, Z_{ij}\right)^2, \qquad \gamma_{ij} = \gamma(R_{ij}) \qquad \text{(III.9)}$$

$$P^{(2)} = e^2 \sum_j \alpha_j \sum_{j'(>i)} \alpha_{j'} \sum_{mn} \Gamma_{jj',mn} \sum_i^I q_i \sqrt{\gamma_{ij}}\, Z_{ij,m} \sqrt{\gamma_{ij'}}\, Z_{ij',n} . \qquad \text{(III.10)}$$

In the case of one charge (I = 1), Eqs. (III.9-10) become

$$P^{(1)} = -\sum A_j \gamma_{ij} Z_{ij}^2 \qquad \text{(III.9')}$$

$$P^{(2)} = e^2 \sum_j \alpha_j \sum_{j'(>j)} \alpha_{j'} \sum_{mn} \Gamma_{jj',mn} \sqrt{\gamma_{ij}}\, Z_{ij,m} \sqrt{\gamma_{ij'}}\, Z_{ij',n} . \qquad \text{(III.10')}$$

The description of the charge delocalization between two or more atoms is complicated by the dynamics of the charge motion.[57] Let us consider, for

example, a rare gas cluster ion R_n^+. In small R_n^+ clusters the charge is delocalized between three atoms which constitute the ionic core of the cluster (for a discussion of the structure of the R_n^+ clusters, see Section V), whereas other R atoms are left netural or almost neutral. In many other ionic clusters, such as heteronuclear rare gas clusters $Ar_2^+Ne_n$ or aromatic cations with rare gas atoms M^+R_n,[51] it is also possible to distinguish between the ionic core and neutral atoms which are polarized by the ionic core. The charge delocalization in a positive ionic cluster core (molecule) can be described as a motion of a positive hole with some characteristic time of the hole "jump" between adjacent atoms. This time is on the order of h/E, where E is the coupling energy responsible for charge delocalization. Since neutral atoms and/or molecules also need some time to be polarized, the interaction between them and the delocalized charge is influenced by dynamical effects. When the polarization time is much smaller than the characteristic time of the hole motion (adiabatic polarization), then the polarization will follow the hole motion and the polarization energy will become an average of the polarization energies of all hole localizations. Thus in the case of one neutral atom polarized by an ionic molecule or cluster core, the adiabatic polarization in the point-dipole approximatation is

$$P_a = \frac{1}{2} \alpha \sum_i a_i^2 F_i^2 \quad , \tag{III.11}$$

where a_i^2 is the hole population at the i-th atom and F_i is the field generated by a hole located at the i-th atom. In the opposite case, where the polarization time is much larger than the characteristic time of hole motion, (diabatic polarization), the neutral atom will be polarized by the average field,

$$P_d = \frac{1}{2} \alpha \left(\sum_i a_i^2 F_i\right)^2 \quad . \tag{III.12}$$

As an example of a system (unrealistic, unfortunately) which demonstrates a dramatic difference between two kinds of polarization, we suggest an ionic

ring with a neutral atom at the ring center. For the diabatic case it is zero, whereas for the adiabatic case it is $-C\gamma(R)/R^4$, R being the ring radius.

In the simple case of a diatomic ion and the neutral atom which it polarizes, the general (from a dynamical point of view) expression for the polarization energy is

$$P = -\frac{\alpha}{4(\epsilon + 2h)} \left[\epsilon(\gamma_i F_i^2 + \gamma_2 F_2^2) + h(\sqrt{\gamma_2 F_1} + \sqrt{\gamma_2 F_2})^2\right] , \qquad \text{(III.13)}$$

where ϵ is the atomic S → P excitation energy which determines the atom polarization time, and h is the interatomic exchange energy of the hole motion which determines the hole motion characteristic time. According to Eq. (III.13) the adiabatic ($\epsilon >> h$) and the diabatic ($\epsilon << h$) polarization energies are

$$P_a = -\frac{1}{4}\alpha\,(\gamma_1 F_1^2 + \gamma_2 F_2^2) \qquad \text{(III.14)}$$

$$P_d = -\frac{1}{8}\alpha\,(\sqrt{\gamma_1 F_1} + \sqrt{\gamma_2 F_2})^2 \quad . \qquad \text{(III.15)}$$

The transition from the adiabatic to diabatic polarization takes place at $h \simeq 0.5\epsilon$, so that the more accurate polarization criteria are

$$\epsilon >> 2h, \quad \text{adiabatic} \qquad \text{(III.16)}$$

$$\epsilon << 2h, \quad \text{diabatic} \quad . \qquad \text{(III.16')}$$

It is reasonable to assume that in more complicated systems these criteria will be valid as well, at least roughly.

Dealing with ionic clusters, we need to know whether to use the adiabatic (III.11) or diabatic (III.12) expressions. For most ionic clusters, the adiabatic condition (III.16) is fulfilled, since the exchange term h is usually on the order of 1-2 eV, whereas the excitation energy ϵ is generally on the order of 10 eV. In the literature, however, the model calculations are usually performed within the diabatic approximation, i.e., considering the

polarized atom in the average field of a delocalized hole.[51,53,58] According to our estimations for Xe_2^+R (R=He,Ne,Ar) and benzene$^+$-R clusters, the difference between the adiabatic and diabatic polarization energies is noticeable, but not large, accounting for some 10% of the polarization energy.

The adiabatic polarization is expected to take place also in the excited systems with electron transfer, such as the unstable $Cl^-Xe^+Xe_n$ complexes which are formed in irradiated Xe solids.[59] In these complexes the positively-charged hole is delocalized between some number of Xe atoms, like in the ionic Xe_n^+ clusters.[60] The polarization of rare gas atoms by the ionic cores of the Rydberg excited clusters has to be considered in the adiabatic approach as well. However, as will be shown in Section V, the polarization of the rare gas atoms by the Rydberg excited electron should be considered in the diabatic approach.

IV. Diatomics-In-Ionic-Systems (DIIS) Method

As mentioned in the previous section, the ionic charge (hole) in the clusters with charged rare gas atoms is mostly delocalized between two or more atoms. In order to study such systems theoretically, we have previously developed the semiempirical diatomics-in-ionic-systems (DIIS) method.[8] This method makes use of diatomic potentials as initial data for a calculation, but in a different way than the diatomics-in-molecules (DIM) method.

Let us consider a polyatomic system $(A_1A_2...A_J)^+$ consisting of J closed-shell atoms or ions A_i with one electron deficiency (hole) delocalized, generally speaking, between these atoms (ions). For example, the ionic R_n^+ cluster is considered as $(RR...R)^+$ and the neutral (ground-state and excited, with electron transfer) rare gas-halogen cluster R_nX is considered as $(RR...RX^-)^+$. The spin of such systems with one electron deficiency is $S = \frac{1}{2}$. The DIIS wave function is presented as a linear combination of diabatic polyatomic wave functions with a localized hole as

$$\Phi = \sum_{i=1}^{J} \sum_{m=1}^{M_i} C_{im}\Phi_{im} \quad . \tag{IV.1}$$

where Φ_{im} is the diabatic wave function of the configuration $A_1A_2\ldots A_{im}^+\ldots A_J$, with the index m indicating the orientation of the A_i^+ open shell ($M_i = 3$ for a P symmetry A_i^+ shell). For example, the rare gas ionic cluster R_n^+ is described by 3n diabatic configurations $R\ldots R^+\ldots R$ for m = 1,2,3. The R_2X system is described by nine diabatic configurations: R^+RX^-, RR^+X^- and RRX (m = 1,2,3). An ionic cluster consisting of n rare gas atoms and one hydrogen atom $(R_nH)^+$ can also be treated by the DIIS method if the electron affinity of H is neglected and singlet (S = 0) states only are considered. The $(R_nH)^+$ cluster is described by 3n+1 diabatic configurations: $R\ldots R^+\ldots RH$ ($M_i = 3$) and $R\ldots R\ldots RH^+$ ($M_i = 1$).

The diabatic polyatomic wave function Φ_{im} is presented in the DIIS method as an antisymmetrized product of atomic group functions,[43] which are assumed to be exact many-electronic wave functions of individual atoms,

$$\Phi_{im} = \hat{A}\,(\prod_j^J \chi_j\ \chi_{im}), \qquad j \neq i \tag{IV.2}$$

where $\hat{A}$ is the operator which antisymmetrizes electrons belonging to different group functions, like in Eq.(II.1). Since the nonorthogonality of the atomic group functions complicates significantly the energy expression,[61] the zero overlap of atomic orbitals (ZOAO) approximation is usually used in semiempirical methods, in particular in the DIM method.[62,63] The ZOAO approximation allows one to omit the antisymmetrization operator $\hat{A}$, thus rendering the polyatomic wave function (IV.2) as a simple product of atomic group functions. Due to the lack of interatomic electron permutation in the polyatomic function (IV.2) the Hamiltonian of the system can be partitioned into atomic and diatomic terms.[8]

The diagonal matrix elements of the DIIS wave function (IV.1) have the physical interpretation as the energies of the diabatic configurations, i.e., configurations with fixed localization of the hole. Assuming the adiabatic polarization to be valid (see Section III), we include the polarization energy (III.1,9-10) into the diagonal matrix elements. In the ionic clusters with one charge and negligible small dipole-dipole interaction (III.10'), the polarization energy (III.9') is expressed in a pairwise way and can be

included in the diatomic ion-atom interactions. If all interactions are of pairwise character, then the diagonal matrix elements are presented as a sum of atomic energies and diatomic interactions as

$$H_{im,im} = \sum_j W_j + \sum_{j_1} \sum_{j_2(>j_1)} W_{j_1} W_{j_2} + U_i + \sum_j U_{im,j}, \qquad j,j_1,j_2 \neq i \qquad \text{(IV.3)}$$

where W_j is the energy of the closed-shell atom A_j, $W_{j_1 j_2}$ is the diatomic potential between two closed-shell atoms A_{j_1} - A_{j_2}, U_i is the energy of the open-shell atom A_i^+ with an electron deficiency, and $U_{im,j}$ is the diabatic diatomic potential between the m-oriented open-shell atom A_{im}^+ and the closed-shell atom A_j. In the case of ionic clusters, the closed-shell atoms A_j are neutral and the open-shell atoms A_i^+ are the ions. However, in other systems the open-shell atom with electron deficiency A_{im}^+ might not be an ion but rather a neutral atom, such as $(Cl^-)^+ = Cl$.

In clusters with more than one charge, such as those with R^+ and X^- ions, Rydberg-excited clusters (positive atomic core and excited electron) or multiply-charged ionic clusters,[64-65] as well as in any systems with non-negligible dipole-dipole interactions, the polarization energy cannot be expressed in a pairwise way. In this case the polarization energy has to be singled out into a separate term P_i, and the DIIS diagonal matrix elements are expressed as a sum of P_i and diatomic diabatic (Coulombic) potentials $\bar{U}$ as

$$H_{im,im} = \sum_j W_j + \sum_{j_1} \sum_{j_2 (>j_1)} \bar{U}_{j_1 j_2} + U_i + \sum_j \bar{U}_{im,j} + P_i, \qquad j,j_1,j_2 \neq i \quad \text{(IV.4)}$$

where $\bar{U}_{j_1 j_2}$ are the Coulombic potentials between pairs of closed shell atoms, and $\bar{U}_{im,j}$ are the Coulombic potentials between open-shell atoms (with a hole) and closed-shell atoms. The ion-atom Coulombic potentials are obtained by excluding the polarization term (III.7) from the potentials $W_{j_1 j_2}$ and diabatic potentials $U_{im,j}$,

$$\bar{U}_{j_1 j_2} = W_{j_1 j_2} - A_{j_2} \gamma(R_{j_1 j_2}) / R_{j_1 j_2}^4 \qquad \text{(IV.5)}$$

$$\bar{U}_{im,j} = U_{im,j} - A_j\gamma(R_{ij})/R^4_{im,j} \quad . \tag{IV.6}$$

In Eq. (IV.5) the j_1-th atom is an ion, and in Eq. (IV.6) the i-th atom is an ion. If both atoms are neutral, the Coulombic potentials coincide with the diatomic potentials W and U. The polarization term P_i is determined by Eqs. (III.9-10) with charges $q_i = 1$ (the index i in Eqs. (III.9-10) is for charged atoms, whereas in this section it is for the hole localization).

The off-diagonal matrix elements H_{im_1,im_2} between the diabatic states with the same hole localization i but different orientation m are expressed by the diabatic diatomic potentials $U_{im,j}$, whereas the off-diagonal elements between the diabatic states with different hole localizations are expressed by the diatomic exchange terms V [8]

$$V_{i_1m_1,i_2m_2} = \int dv\ \chi_{i_1}\chi_{i_2m_2}\ h_{i_1i_2}\ \chi_{i_1m_1}\chi_{i_2} \quad , \tag{IV.7}$$

where dv is a differntial volume element, $h_{i_1i_2}$ is the Hamiltonian of the diatomic interaction, and χ_i and χ_{im} are the group functions of the closed-shell and open-shell atoms, respectively. The transformation of the potentials U and exchange terms V between m-oriented orbitals to the Σ and Π potentials and exchange terms is described in Reference 8.

The diatomic potentials $W_{j_1j_2}$ between closed-shell atoms are taken from empirical studies or *ab initio* calculations. The diabatic potentials $U_{im,j}$ between open-shell (i) and closed shell (j) atoms, such as R^+-R, have to be calculated since only adiabatic potentials, such as $W_{R_2^+}$, are the physically defined values. The calculation of the diabatic potentials can be performed by considering the diatomic fragments within the DIIS approximation and solving the inverse problem of the 2 × 2 matrix eigenvalues, i.e., calculating the matrix elements for given eigenvalues. In the case of the homonuclear fragment R_2^+, the 2 × 2 matrix of the fragment is

$$\begin{vmatrix} U-E & V \\ V & U-E \end{vmatrix} = 0 \quad . \tag{IV.8}$$

where U is the R^+-R diabatic potential and V is the exchange term in the $(R^+-R)-(R-R^+)$ coupling. Substituting into Eq. (IV.8) the known adiabatic potentials $E^{(1)} = {}^2\Sigma_u$ and $E^{(2)} = {}^2\Sigma_g$, we can easily find the diabatic potential U and the exchange term V for Σ symmetry. In the same way, U and V of Π symmetry are found. For the case of heteroatomic fragments there are two different diabatic potentials, so that one needs an extra empirical or *ab initio* value to solve the inverse eigenvalue problem and to find the diabatic potentials U and the exchange term V. For such an extra value it is possible to use the diatomic static or transition dipole moment.[8,39] After the diabatic potentials U and the exchange terms V of all diatomics fragments are determined, the Hamiltonian matrix elements (presented in Reference 8) can be calculated, and the wave function (IV.1) and its energy spectrum can be found.

In the wave function (IV.1), the spin-orbit coupling is not taken into account, at least directly. However, the energy level shifts resulting from this coupling can be incorporated into the system energy indirectly by taking as the input of the DIIS calculation the empirical or *ab initio* potentials with spin-orbit coupling. By presenting the wave function (IV.1) without spin-orbit coupling, we are losing some of the excited states and are excluding from our consideration the S-P mixing effect in the collinear configuration.

V. Ionic Rare Gas Clusters

The ionic rare gas clusters R_n^+ have been studied extensively both experimentally and theoretically, particularly recently. In spite of this, the structure of these clusters is still not fully clear. Even for the case of the smallest clusters, R_3^+, the experimental evidence does not allow one to chose definitely the electronic and geometric structure. From a theoretical point of view there are two alternative structures for R_3^+, namely an asymmetrical R_2^+R structure with the charge concentrated on R_2^+ and a structure with the charge distributed among all three atoms. For the case of R_2^+R, where the neutral atom is bound to the R_2^+ molecule by polarization forces

predominately, the triangle geometry is expected to be the most stable one. This triangle geometry was supported by the first quantum chemistry calculation of Ar_3^+ performed by the approximate X_α method.[66] When the charge is delocalized among all three atoms, the exchange interaction contributes significantly to the binding, causing the symmetrical linear geometry to be the most stable one. Such geometry is supported by relatively accurate CI *ab initio* calculations of He_3^+,[67,68] Ne_3^+ [13] and Ar_3^+,[13,69] as well as by DIM[70,71] and other semiempirical[14,72,73] calculations of Ar_3^+ [14,70-72] and Xe_3^+.[14,71,72] In contrast to these findings, a recent Ar_3^+ *ab initio* calculation shows an asymmetrical linear Ar_2^+Ar geometry to be the most stable one.[74] Such geometry, although a little strange from the point of view of an energy balance, can be explained by some contribution of the exchange interaction between the Ar_2^+ dimer and the slightly charged (~ 0.1) outer Ar atom.

The experimental data, obtained mainly for the Ar_3^+ cluster, cannot provide direct evidence about the R_3^+ geometry. The conclusions made by the indirect analysis of the experimental, mostly spectroscopic, data are contradictory. Whereas most of the experimental work confirms the symmetrical linear Ar_3^+ structure,[12,75-81] other works substantiate the asymmetrical Ar_2^+Ar structure, either of triangular[82] or linear[83] geometry. Such discrepancy is due, most probably, to the features of the Ar_3^+ potential energy surface corresponding to a very flat Ar_3^+ potential in the collinear configuration.[72,74] Such a potential causes the vibrational motion to shift, for the most part, the Ar_3^+ configuration far away from the equilibrium configuration, thus significantly affecting the electronic transitions.[84] This problem has been considered in detail in Reference 72 by means of a trajectory study. According to this study the symmetrical linear Ar_3^+ minimum energy configuration alone provides a spectrum close to the experimental one, if one takes into account the vibrational motion. The experimental studies of other R_3^+ clusters, such as He_3^+,[85] Kr_3^+,[86] and Xe_3^+,[87,88] were concentrated mainly on the problems of cluster stability and dynamics of formation, without much consideration of the structure. The interpretation of the Xe_3^+ spectrum obtained in Reference 88 supports the linear geometry of this cluster.

In our calculations[14] performed by the semiempirical DIIS method (see Section IV), the triatomic clusters Ar_3^+ and Xe_3^+ have a symmetrical linear equilibrium configuration, in accordance with most of the other calculations.[16,69-73] For the interatomic distances at the Ar_3^+ equilibrium configuration, our calculation gives 2.59 Å, exactly the same as another semiempirical calculation[72] but slightly less than an *ab initio* calculation (2.62 Å).[69] The cluster charge is shared equally between the inner and two outer atoms (Figure 1), like in Reference 72. In the excited $^2\Pi_g^+$ state the charge is localized on the outer atoms, which is confirmed by an experimental study.[81] The $Ar_3^+ \rightarrow Ar_2^+ + Ar$ dissociation energy is found to be equal to $D_e = 0.20$ eV (Table 4), close to the experimental values of 0.22 eV[13,82] and 0.10 eV.[89] (Throughout the manuscript, we shall refer to the theoretical well depths D_e as dissociation energies, since the zero-point vibrational energies are typically very small, i.e., ~ 0.001-0.01 eV.) Other calculations give results a bit lower than our dissociation energy, namely 0.18 eV,[13] 0.16[69] 0.20 eV,[71] 0.17 eV[72] and 0.15 eV.[74] The $\Sigma_u \rightarrow \Sigma_g$ transition energy and transition moment in the equilibrium configuration are found to be equal to 2.26 eV and 0.8 D_e, respectively, close to other theoretical values.[13,72] According to our calculations for the triatomic Xe_3^+ cluster, like for Ar_3^+, 50% of the charge is concentrated at the central atom (Figure 2), in accordance with other calculations,[13,73] and the Xe-Xe separation is equal to 3.30 Å (3.47 Å in Reference 13 and 3.32 Å in Reference 72). The $Xe_3^+ \rightarrow Xe_2^+ + Xe$ dissociation energy is found to be 0.20 eV (Table 5), a little lower than the experimental value of 0.27 eV[87] but halfway between the theoretical values of 0.12 eV[13] and 0.36 eV.[73] For the $\Sigma_u \rightarrow \Sigma_g$ transition energy we obtain 1.87 eV, a bit higher than in Reference 13 (1.6 eV).

The most stable Ar_4^+ cluster, according to our DIIS calculation, is formed by a collinear Ar_3^+ ion and almost neutral (q = 0.002) Ar atom separated from the nearest charged atom by 3.68 Å (Figure 1). The dissociation energy of the $Ar_4^+ \rightarrow Ar_3^+ + Ar$ detachment process is found to be equal to $D_e = 0.047$ eV, a typical energy of the polarization attraction (Table 4). According to the DIM calculation,[71] the most stable configuration (dissociation energy $D_e = 0.043$ eV) has a structure Ar_3^+Ar, like in our calculation, but with a

linear geometry. In our calculation the linear asymmetrical Ar_3^+Ar cluster presents a metastable structure with a dissociation energy of 0.031 eV only. Since the differences in the energies of the isomeric Ar_4^+ structures are small, most probably beyond the accuracy of the semiempirical calculations, it is really difficult to conclude which geometry is the most stable one. The more important finding of the semiempirical calculations[14,71,72] is the asymmetrical Ar_3^+Ar structure of the Ar_4^+ cluster. Due to this structure the Ar_4^+ excitation spectrum is expected to be similar to the Ar_3^+ spectrum. In addition to the asymmetrical Ar_3^+Ar structures, we find also a metastable symmetrical Ar_4^+ configuration with the geometry of an equilateral pyramid with a separation of 2.836 Å between every two atoms (Figure 1, Table 4). The energy of this fully symmetrical structure is only 0.01 eV above the energy of the most stable Ar_4^+ configuration. In the case of xenon clusters just the symmetrical equilateral pyramid (Xe detachment energy as large as D_e = 0.203 eV) is found to be the most stable configuration of the Xe_4^+ cluster (Figure 2).[14] The most stable asymmetrical Xe_3^+Xe configuration in our calculation has a bent structure and the Xe detachment energy of 0.079 eV, much smaller value than that of the symmetrical pyramid. This asymmetrical configuration is separated from the configuration of the symmetrical pyramid by a high barrier of approximately 0.3 eV. In contrast to our results, in Reference 73 the most stable Xe_4^+ structure (Xe detachment energy of 0.159 eV) is a symmetrical linear geometry. In our calculation the symmetrical linear Xe_4^+ cluster is a metastable configuration with a Xe detachment energy of 0.069 eV only. The three Xe_4^+ configurations, namely the symmetrical pyramid, the symmetrical linear structure and the asymmetrical (bent) Xe_3^+Xe structure, are expected to have different spectrum features, so that they can be distinguished by experimental spectral studies.

In the R_n^+ ($n > 3$) clusters, the charge is supposed to be localized at an ionic core consisting of a few R atoms. This ionic core is surrounded by neutral or almost neutral atoms which are attracted to the charged core by polarization and, to a lesser degree, by dispersion forces (Tables 4 and 5). The main problem which has been intensively discussed in many experimental and theoretical works is the size and structure of the ionic cores. The simplest

model of one atom ionic core[90] is unrealistic, as the rare gas ions R^+ are chemically active and are able to form diatomic molecules R_2^+ or R_n^+ clusters where charge is shared by all cluster atoms. The strongly-bound (D_e ~ 1 eV) diatomic molecules R_2^+ provide the simplest realistic model for an ionic core.[91,92] Since these molecules can combine, as noted above, with more R atoms forming relatively strongly-bound (D_e ~ 0.2 eV) ionic trimers or weakly-bound R_4^+ clusters, the three- and four-atomic ionic cores should be considered as an alternative to the two-atomic ionic cores. Although in the gas-phase these clusters are more stable than the R_2^+ molecules, the stability inside the cluster is not obvious, as the energy of the polarization and dispersion interaction between an ionic core and neutral atoms and between neutral atoms themselves is on the same order as the cluster dissociation energy. The delocalization of the charge on more atoms decreases the system energy but decreases also the attractive polarization energy, which imposes limits on the charge spread. This tendency of the charge localization on a small number of atoms is reinforced by the relaxation shift of atoms along the lines of attractive forces and the formation of a stable ionic core. The *ab initio* calculation of small (n = 4-7) He_n^+ clusters[60,69] shows that the most stable ionic core has the structure of a linear symmetrical trimer, similar to the free He_3^+ cluster. According to semiempirical calculations of Ar_n^+ [14,71] and Xe_n[14,71,73] ionic clusters, the ionic core may consist of either three or four atoms. As shown in Reference 73, the linear symmetrical trimer and tetramer cores yield very similar energies for numerous, almost degenerate, isomers of Xe_n^+ clusters. Slightly different results are obtained for Ar_n^+ and Xe_n^+ clusters in Reference 71, where the linear symmetrical trimer core is found to be more stable in small clusters (n < 13) and the linear symmetrical tetramer core to be more stable in larger (n > 13) ones. On the basis of this finding, the last model calculation of Ar_n^+ (n = 3-27) clusters was performed for both trimer and tetramer (linear symmetrical) ionic cores.[93] In our calculation,[14] in contrast to the results of References 71 and 73, the most stable Xe_n^+ clusters are formed by a symmetrical equilateral Xe_4^+ core.

The spectroscopic, photodissociation, and ionization studies of R_n^+ clusters are contradictory in their conclusions concerning the structure of

the ionic cores. In some of this work the conclusion is made that in Ar_n^+ clusters the Ar_2^+ dimer presents the core.[91,94,95] In other works the experimental evidence is interpreted in favor of the trimer core in Ar_n^+ [15,75,81] (for a critique of the interpretation of Reference 81, see Reference 96) and in Xe_n^+ [97] clusters. Recent studies, however, present more evidence about the dependence of the ionic core structure on the cluster size.[77,88,96] According to this work, the charge is located on a trimer core in small clusters ($n < 13$ in Reference 77) and is spread out on a tetramer core in larger clusters, in accordance with the DIM calculation.[71] The rise of the charge delocalization with the increase of the cluster size is, however, somewhat contradictory with the fact that in solid argon the ionic charge is concentrated on a dimer.[98] The conclusions about the structure of the ionic core are based mainly on the comparison of the spectroscopic (and some other) properties of the ionic clusters R_n^+ ($n > 4$) with the corresponding properties of the R_2^+ molecule and the R_3^+ or R_4^+ free ionic clusters. It is important to note that such comparison may lead to incorrect conclusions, as the spectroscopic properties depend on the charge distribution not only in the ground state but also in the excited states. Even if the charge is concentrated in the ground state on a trimer core, for example, in the excited state the charge may be partly transferred to other (neutral in the ground state) atoms, which affects the excitation spectrum. This point is supported by our semiempirical calculation of the excitations of small Ar_n^+ and Xe_n^+ clusters.[14]

The size and structure of ionic cores affect the stability of the R_n^+ clusters. The mass-spectroscopic studies of the ionic R_n^+ clusters show that some of these clusters are much more abundant than others, giving rise to so-called magic numbers. These numbers found in different works are not always the same. For example, in He_n^+ clusters it is not clear whether $n = 4$ is the magic number or $n = 7,10,14,30$.[99-101] In argon and xenon clusters $n = 13$ is found as the magic number, like in the neutral clusters with the ioosahedral symmetry.[92,90,102] This $n = 13$ argon cluster is not found, however, as the magic one in Reference 103. In considering the abundance of the ionic clusters, we have to keep in mind not only the stability of such clusters but

also the reltive stability of neutral clusters where ionization produces the ionic clusters. After the cluster is ionized and the initial ionic core is formed, the cluster relaxation to the stable ionic core gives rise to the energy excess which leads to the loss of neutral atoms and dimers.[104] The dynamics of the ionized clusters fragmentation affects significantly the relative abundance of ionic clusters.[105-109]

VI. Rare Gas-Hydrogen Ionic Clusters

Rare gas atoms can form not only the homonuclear clusters R_n^+ considered in the previous section but also ionic heteronuclear clusters consisting either of different rare gas atoms or rare gas atoms and molecules or valence-active atoms. The charge distribution and the structure of heteronuclear ionic clusters depend strongly on the relation between the ionization potentials of the atoms involved. If the cluster is formed by atoms and molecules with very different ionization potentials, the charge is obviously localized on the particles with lower ionization potential. When valence-active atoms are involved, the situation becomes more complicated because of the formation of valence-bonded molecules, such as H_2, H_2^+, H_3^+ and $(RH)^+$ in the case of rare gas-hydrogen clusters.

The rare gas-hydrogen systems $(RH_2)^+$ have been studied in the context of the $R^+ + H_2$ and $R + H_2^+$ chemical reactions.[110-113] The study of the stable rare gas-hydrogen clusters has been concentrated mainly on the case of ArH_3^+,[114] whose structure, by analogy with HeH_3^+,[115] is suggested to be a H_3^+ triangle with Ar at the vertex. This structure is supported by an *ab initio* calculation.[116] The charge is localized on the H_3^+ ion also in $(H_2)_nH_3^+$ ionic clusters,[117,118] since the ionization potential of H_2 (15.34 eV) is much higher than the H ionization potential. The H ionization potential is also much lower than the Ne ionization potential, so that in the ionic clusters Ne_nH^+ the atom H is expected to bear the charge, what is confirmed by an *ab initio* calculation.[119] The rare gas atoms are also usually neutral (or almost neutral) in clusters which they form with ionic molecules, such as N_2^+ [120] or aromatic cations.[51,53,121,122] In all these systems the charge is

strongly localized and the particles are kept together mainly by polarization forces. The heteronuclear ionic clusters with rare gas atoms has recently attracted much interest. The new (cluster) class of reactions[123-125] suggest possible practical application of the heteronuclear ionic clusters.

Considering the structure of rare gas-hydrogen ionic clusters by the semiempirical DIIS method,[14] we decided to look at Ar and Xe, since they are expected to form different kinds of clusters with H, as the H ionization potential (13.6 eV) lies between the ionization potentials of Ar and Xe (Table 1).

According to the results of our semiempirical DIIS calculation, the argon-hydrogen $(Ar_nH)^+$ clusters are formed by an $(ArH)^+$ molecule and n-1 neutral Ar atoms which are attracted to the ionic molecule by polarization forces (Table 5). The $(ArH)^+$ ion is a strongly-bound molecule with dissociation energy of 4.055 eV and equilibrium distance of 1.266 Å.[22,25,126] The neutral Ar atoms are located on the H side of the $(ArH)^+$ molecule, as the H atom bears larger (+0.569) charge than the Ar atom. The $Ar(ArH)^+$ cluster has a bent geometry with the neutral Ar atom at a distance of 2.81 Å from H. In the $Ar_n(ArH)^+$ (n = 2-4) clusters, the neutral Ar atoms are located symmetrically around the $(ArH)^+$ axis. The $(ArH)^+$ molecule is only slightly affected by the surrounding neutral atoms in the cluster. In the sequence of $Ar_k(ArH)^+$ clusters, the charge is shifted slightly from the Ar atom to the H atom, but the interatomic distance is practically not changed. The energy of the Ar detachment in the $Ar_k(ArH)^+$ clusters is decreasing with k from 0.19 eV for k = 3 to 0.09 eV for k = 6 (Table 6). The electronic spectrum of these was found to be practically identical to the free $(ArH)^+$ spectrum.

The results of our semiempirical calculation contradict those of an *ab initio* calculation,[127] indicating the $(ArH)^+$ molecule to be strongly affected by other Ar atoms. The simplest argon-hydrogen cluster has a linear ArHAr asymmetric structure with the Ar-H distances of 1.42 Å (compared to 1.266 Å in a free $(ArH)^+$ molecule) and 1.0 Å (compared to 2.8 Å in our calculation). Also, in larger $(Ar_kH)^+$ clusters one of the Ar atoms is bound more strongly with the H atom than others, but not as strongly as in a free $(ArH)^+$ molecule. The *ab initio* results look somewhat strange for two reasons.

First, the hydrogen is a one-valence atom and cannot provide a valence bond with two atoms. Second, the neutral Ar atom polarization energy is on the order of 0.2 eV, a much smaller value than the $(ArH)^+$ dissociation energy.

The argon-hydrogen molecule ionic cluster $(ArH_2)^+$ has three asymptotic states, $Ar^+ + H_2$, $Ar + H_2^+$ and $H + (ArH)^+$, with dissociation energies of 4.76 eV, 4.95 eV and 6.215 eV, respectively. The most stable cluster can be formed by the $(ArH)^+$ molecule and H atom. However, according to our calculation, the polarization attraction of the H atom to the ionic molecule is so weak that the H atom and $(ArH)^+$ are not attached. The lowest quasistable $(ArH_2)^+$ cluster has a triangle geometry and is formed by the H_2^+ ion and almost neutral (q = +0.02) Ar atom located symmetrically with respect to both H atoms. The $Ar + H_2^+$ dissociation energy is found to be 0.19 eV. The quasistable ArH_2^+ cluster is separated from the stable $(ArH)^+ + H$ state by a barrier of, roughly, 0.75 eV. The structures of the quasistable $Ar_nH_2^+$ ($k < 6$) clusters are similar to that of the ArH_2^+ cluster, i.e., the almost neutral Ar atoms are located in the plane perpendicular to the H_2^+ axis.

The xenon-hydrogen ionic clusters $(Xe_nH)^+$, like the argon-hydrogen clusters, are formed by neutral Xe atoms and the $(XeH)^+$ ionic molecule. The $(XeH)^+$ molecule is a strongly-bound system with dissociation energy around 4 eV and equilibrium distances of 1.6 Å.[24-27] In the $Xe_k(XeH)^+$ clusters, in contrast to the $Ar_k(ArH)^+$ clusters, the neutral Xe atoms are located on the Xe side of the $(XeH)^+$ molecule, since in this molecule the rare gas atom bears most of the charge. The $Xe(XeH)^+$ cluster is found to have a linear XeXeH geometry. The Xe detachment energy in the $Xe_k(XeH)^+$ clusters is low, 0.04-0.08 eV only. The $(Xe_2H)^+$ clusters have been studied experimentally in Xe solids.[128] The structures of these clusters are found to be different from those obtained by us for the gas phase.

The xenon-hydrogen molecule $(XeH_2)^+$ ionic clusters are expected to be formed by Xe^+ ion and a neutral H_2 molecule, whose ionization potential is about 3.3 eV higher than that of Xe. The DIIS calculation, however, shows the existence of a strongly-bound linear $(XeHH)^+$ cluster with some transfer of the charge from the Xe^+ ion to the next H atom, which bears a small charge of +0.044. The Xe-H distance in this cluster is 1.79 Å, 0.18 Å larger than in

the free $(XeH)^+$ molecule, and the H-H distance is 0.81 Å, 0.07 Å larger than in the free H_2 molecule. The energy of the $Xe^+ + H_2$ dissociation of the cluster is large, 0.456 eV. The electronic structure of the $(XeHH)^+$ cluster can be described as a superposition of the Xe^+HH and $(XeH)^+H$ configurations. The existence of the valence bound $(XeHH)^+$ cluster can be detected experimentally by studying its spectrum, which is found to be very different from that of the H_2 and $(XeH)^+$ molecules. The structure of the $(Xe_kH_2)^+$ clusters with more than one Xe atom is quite different from the $(XeHH)^+$ structure. The $(Xe_kH_2)^+$ clusters are formed by ionic H_k^+ clusters and a neutral H_2 molecule which is bound to the charged atoms by polarization forces. The $Xe_k^+ + H_2$ dissociation energy of the $Xe_k^+H_2$ clusters is about 0.1 eV. Due to the interaction with the H_2 molecule, the Xe_k^+ geometry in the $Xe_k^+H_2$ clusters is different from that of the free Xe_k^+ clusters.

In the semiempirical DIIS calculation of the rare gas-halogen ionic clusters, empirical or *ab initio* potentials of the following diatomic fragments were used: R_2, H_2, RH, R_2^+, H_2^+ and $(RH)^+$, R = Ar,Xe. These diatomic potentials were fitted by simple analytical expressions presented in Reference 14.

VII. Rare Gas-Halogen Systems with Electron Transfer

The rare gas-halogen quasistable molecules with electron transfer R^+X^- and $R_2^+X^-$ have attracted much interest, particularly because of their lasing properties.[129-136] These excited molecules are obtained by electron impact or by optical irradiation of rare gas-halogen mixtures. The quasistable molecules $R_2^+X^-$ have also been detected in the condensed phase.[59,137-143] In a pure rare gas matrix, for example in Xe solid doped with Cl_2 and HCl, near-UV irradiation produces the quasistable triatomic molecules, whereas in a mixed rare gas host, such as Kr and Ar solid with a Xe admixture, the diatomic Xe^+Cl^- molecules are formed.[59] The R^+X^- and $R_2^+X^-$ molecules in solids, in contrast to the gas phase, interact with other host rare gas atoms to form some systems which can be described as $R_n^+X^-$ $(n > 2)$ clusters.[141,142] More than two rare gas atoms are also involved in solids in the excitation to the

states with electron transfer from R to X atom, which is well demonstrated by excitation spectra.[60]

These rare gas-halogen molecules with electron transfer have also been studied theoretically. *Ab initio* calculations of diatomic molecules have been performed for XeX, X = F,Cl,Br,I, in both ground (neutral configuration) and excited (ionic configuration R^+X^-) states. *Ab initio* calculations of the triatomic R_2X molecules have been performed for R_2F, R = Ar,Kr,[144] and Xe_2Cl.[145] Semiempirical DIM calculations of Kr_2Cl and R_2F, R = Ne,Ar,Kr,[146] and Xe_2Cl[147] have been performed for the excited $R_2^+X^-$ (ionic) configurations but without taking into account the coupling with the ground state (neutral) configuration.

The R_nX molecules and clusters in both ground state (neutral) and excited (ionic) configurations can be described as systems with one hole in their closed-shell atoms. Such systems, as discussed in Section IV, can be considered by the semiempirical DIIS method. Since the R_nX systems in the excited states with electron transfer (ionic configuration $R_n^+X^-$) have two charges, the polarization energy is not of pairwise character, which makes the calculation more complicated (see Section III). It is important to note that due to the coupling between the neutral and ionic configurations, some small electron transfer from R to X takes place also in the neutral state (see Section II), with the electron transfer in the excited $R_n^+X^-$ states not being 100%. The DIIS method takes into account just this coupling, opposite to the DIM method in the version used for the calculation of the R_2X molecules.[146,147] The DIIS method has been applied by us for the semiempirical calculations of Xe_nCl[8,60] and Xe_nHCl[39] clusters in the gas phase[8,39] and solids.[39,60]

The DIIS calculation[8] of the triatomic quasistable molecule $Xe_2^+Cl^-$ provides potential energy surfaces similar to those of the DIM calculation.[146,147] Unlike DIM, the DIIS calculation provides also the dipole transition moments between excited and ground states. The lowest quasistable excited state, $4^2\Gamma$, according to the DIIS calculation, has a configuration of an isosceles triangle with the Xe-Cl-Xe angle of 60.4° and Xe-Cl distance of 3.23 Å, 0.16 Å larger than in the quasistable diatomic Xe^+Cl^- excimer. The

Xe-Xe distance is 3.25 Å, almost the same as in the ionic Xe_2^+ molecule. Qualitatively, the excited trimer can be described as a Xe_2^+ molecule and Cl^- ion which are attracted to each other by a Coulombic force. The coupling between the ionic and neutral configuration decreases slightly the Xe_2^+ and Cl^- charge, which in the $4^2\Gamma$ state is found to be 0.964 and -0.964, respectively. The coupling decreases the energy of the $4^2\Gamma$ quasistable trimer by 0.07 eV and increases the ground-state energy in the geometry of the quasistable trimer by 0.1 eV. The energy of the transition from the quasistable $4^2\Gamma$ state to the $1^2\Gamma$ ground state is found to equal 2.56 eV (485 nm), which is close to the center of the $4^2\Gamma \rightarrow 1^2\Gamma$ emission band.[136] The $4^2\Gamma \rightarrow 1^2\Gamma$ transition moment has a sharp minimum in the $Xe_2^+Cl^-$ equilibrium geometry.

A quasistable molecule with rare gas-halogen electron transfer is found also in the Π-symmetry $4^2\Gamma_\Pi$ state. Like in the Σ-symmetry $4^2\Gamma$ state, the Π-symmetry quasistable molecule has the geometry of an isosoeles triangle, but with a much larger Xe-Cl-Xe angle of 85°. The Xe-Cl distance in this trimer is 3.13 Å, shorter than in the $4^2\Gamma$ state, whereas the Xe-Xe distance is much larger than in the $4^2\Gamma$ state, so that the $4^2\Gamma_\Pi$ quasistable molecule cannot be considered as formed by a Cl^- ion and Xe_2^+ ionic molecule. The energy of the quasistable $4^2\Gamma_\Pi$ molecule is 0.8 eV higher than that of the lowest quasistable $4^2\Gamma$ molecule.

There are two possible models of the structure of quasistable $Xe_n^+Cl^-$ ($n > 2$) clusters. First, they can be formed by the $Xe_2^+Cl^-$ trimer and neutral Xe atoms, which are attracted to the trimer by polarization forces. The polarization forces in this case are expected to be weaker than in the case of ionic clusters (see Sections V and VI), since the $Xe_2^+Cl^-$ trimer is not a charged particle but a particle with a dipole moment. The second possibility is the formation of the $Xe_n^+Cl^-$ cluster by the Cl^- ion and the ionic Xe_n^+ cluster, especially the relatively stable Xe_3^+ cluster which, in a free state, has most probably a symmetrical linear structure (see Section V). According to the results of our calculation for $n = 3$, the first possibility is realized, and the most stable $Xe_3^+Cl^-$ cluster has the $XeXe_2^+Cl^-$ structure with the neutral Xe atom located symmetrically above the triangle $Xe_2^+Cl^-$ plane at a distance of 3.52 Å from the Cl atom and 4.41 Å from two charged Xe atoms.

This Xe atom is not completely neutral, but the charge it bears is negligibly small, +0.005 only. The energy of the neutral Xe atom detachment is relatively large, 0.11 eV. The $XeXe_2^+Cl^-$ vertical transition energy to the ground state is 2.48 eV, close to the $Xe_2^+Cl^-$ transition energy of 2.56 eV, which makes it difficult to detect the $XeXe_2^+Cl^-$ clusters by their emission energy. The less stable cluster (Xe detachment energy of 0.06 eV) can be described as formed by the Xe_3^+ cluster and Cl^- ion; however, the Xe-Xe distances in this $Xe_3^+Cl^-$ cluster (3.58 Å) are much larger than in the free Xe_3^+ cluster (3.38 Å), and consequently the three Xe atoms do not form a valence bond system. The Cl^- ion is located symmetrically with a distance from the central Xe atom of 3.33 Å. Like in the n = 3 case, the most stable $Xe_n^+Cl^-$ (n > 3) clusters are formed by the $Xe_2^+Cl^-$ trimer and almost neutral n-2 Xe atoms. The structure of the n = 12 cluster, for example, is $Xe_{10}Xe_2^+Cl^-$. The $Xe_2^+Cl^-$ trimer in this cluster is a little bit deformed, and its Xe-Xe and Xe-Cl distances (equal one to another) are larger by 0.04-0.06 Å than in the free $Xe_2^+Cl^-$ cluster. This deformation of the $Xe_2^+Cl^-$ trimer is mainly due to some loss of the positive charge, which is transferred to the ten so-called neutral atoms which bear together 4.3% of the positive charge.

The $Xe_{12}^+Cl^-$ system is of great interest in regard to Xe solids doped by Cl-containing molecules.[49,59,148] These molecules, usually Cl_2 or HCl, are dissociated by irradiation producing free Cl atoms which replace Xe atoms and form a $ClXe_{12}$ cage with the Cl atom in the middle. The photon excitation of this cage leads to electron transfer from the Xe atoms to the Cl atom and the formation of the spherically symmetrical or almost symmetrical $Xe_{12}^+Cl^-$ complex which, in accordance with the results obtained for the $Xe_{12}^+Cl^-$ cluster, is unstable and tends to form a $Xe_{10}Xe_2^+Cl^-$ complex. According to the DIIS calculation of this complex in its equilibrium geometry, the Cl^- atom is shifted from the center of the Xe matrix cage by 1.12 Å forming with two Xe atoms the $Xe_2^+Cl^-$ trimer. The trimer has the shape of an isosoeles triangle with the quasistable Xe-Cl-Xe angle as 60.2°, each Xe-Cl distance as 3.30 Å, and the Xe-Xe distance as 3.31 Å. These distances are larger than in the free $Xe_2^+Cl^-$ cluster (3.22 Å and 3.25 Å, respectively) but are close to the interatomic distances in the $Xe_{10}Xe_{12}^+Cl^-$ cluster (3.29 Å). The ionic charge

of the Cl^- ion is -0.97, almost the same as in the gas-phase $Xe_2^+Cl^-$ molecule (-0.964). The positive charge is partly delocalized, so that the common charge of the two Xe atoms of the trimer is +0.932, whereas +0.038 of the positive charge is distributed among the other ten atoms of the cage. One of these atoms which carries most of this charge, +0.021, is shifted further from the Cl^- ion by 0.1 Å. Nine other Xe cage atoms are located at the same points as in the ground (neutral) state. The transition from the quasistable $Xe_2^+ Cl^-$ configuration to the ground state has a large transition moment of 2.41 D_e. The vertical transition energy is 2.95 eV, 0.21 eV smaller than the gas-phase $Xe_{12}^+Cl^-$ transition energy. The experimental value for the shift of the $Xe_2^+Cl^- \rightarrow Xe_2Cl$ transition energy in the solid, compared to the gas phase, is larger, namely 0.38 eV.[59] The calculation of the potential curves for the inner motion of the atoms inside the $Xe_{12}^+Cl^-$ trimer allows us to estimate vibrational excitations, which are found to be small, 0.034 eV and 0.012 eV. The vibrational motion broadens by some 0.28 eV the energy of the transition to the repulsive ground state and affects significantly the shape of the emission spectrum.

The rare gas atoms are known to form van der Waals (vdW) clusters with HCl molecule.[37,149-150] These clusters can be excited, in particular in the rare gas solids, to states with electron transfer forming quasistable complexes similar to the $R_n^+X^-$ complexes considered above. In order to study the possibility of the formation of such quasistable complexes, we have performed DIIS calculations for Xe_nClH systems.[39] According to our results, strongly bound XeClH quasistable molecules with electron transfer are formed in several excited states and surprisingly even in the ground state (Figure 3). The ground state molecule is found to have a collinear $(HXe)^+Cl^-$ configuration of Σ symmetry with a very large dipole moment of 15 D_e. The energy of this molecule is low, -0.39 eV, only 4.24 eV higher than the energy of the vdW complex. The $(HXe)^+Cl^-$ molecule is separated from the XeHCl vdW complex by a barrier of 0.41 eV and consequently can be detected at low temperatures. In the first excited state the linear Σ symmetry quasistable molecule is also formed, but its structure is different, namely $(XeH)^+Cl^-$. This molecule is separated from the excited $Xe(HCl)^*$ vdW complex by a barrier

of 0.18 eV. The $(XeH)^+Cl^-$ molecule emits in the near-UV (232 μm). In the higher excited states the quasistable molecules have a structure of a Xe^+Cl^- molecule and almost neutral H atom bound to the Xe^+Cl^- molecule by polarization forces. The energy of the H atom detachment from this molecule is relatively large, 0.12-0.18 eV. The Xe^+Cl^-H transition energy to the ground state lies within the limits of 7.3-7.5 eV. In one of the excited states a $(XeH)^+Cl^-$ molecule is formed whose transition energy to the ground state is very low, 0.8 eV. It follows that the quasistable XeHCl molecule provides emission both in the near infrared and in the UV regions and presents an interesting object for spectroscopic study. The quasistable XeHCl molecules with electron transfer can attract more Xe atoms forming quasistable clusters.[39]

In the Xe solids the HCl molecule is photodissociated as a result of valence excitation to the Π state. It is not immediately obvious that after dissociation the H atom is moving to other cages, thus preventing the H-Cl association. However, according to our calculation the H atom, after its detachment from Cl, can surmount a barrier which separates adjacent cages and escape to the bulk, leaving the free Cl atom inside a cage, in accordance with experiments.[59,151]

The excited rare gas-halogen systems with electron transfer are of interest not only in connection with the quasistable systems considered above, but also from the point of view of the electron excitation of the ground-state rare gas-halogen system, such as vdW molecules and clusters or the $ClXe_{12}$ cages in the solid matrix. The problem of the rare gas-halogen systems excitation is of great interest, particularly in solids where the excited species interact with the matrix atoms.[60,151,152] In Xe matrix the Cl atom has some freedom of motion so that the excitation may take place in different localizations of the Cl atom.[49] Since the energy and the transition moment of the excitation is affected by the Cl-Xe atoms interaction, which depends on the Cl atom location, the quantum and thermal motion of Cl determines to some extent the excitation spectrum. The DIIS calculation performed for the ground-state $ClXe_{12}$ system in the Xe matrix shows that the potential energy surface of the Cl atom inside the cage has a broad region of almost constant

potential, with variations within the range of 1 meV. The potential energy surface of the Cl motion has twelve very shallow potential wells which are shifted by 0.5-0.8 Å from the cage center toward the Xe atoms (the Xe distance from the center is 4.33 Å). The barriers between these wells are so low that even quantum effects allow the atom to move inside a relatively wide region of the cage. Thermal effects obviously make the motion stronger and increase the cage region accessible for the atom. Taking into account both quantum and thermal motion, it is possible to determine the probability of the Cl atom location as a function of its location inside the cage. Calculating also the excited states energy and the transition moments for any Cl atom location, it is possible to determine the excitation spectrum. According to the results of this calculation, the 10 K and 80 K spectra do not differ much from other, leading us to the conclusion that the thermal motion does not affect photon absorption to any significant extent. The main contribution to the absorption provides the transition to the second excited state. The spectra demonstrate two wide maxima at 320-340 nm and 270-290 nm which are separated by a deep minimum (Figure 4). The first of these maxima is found to be higher than the second one. The maxima and the lower limit of the absorption are shifted slightly to smaller energies when the temperature increases. Our calculated excitation spectrum is similar to the experimental spectrum, which also demonstrates two broad maxima, roughly in the same wavelength intervals. In accordance with the theoretical prediction, the low-energy maximum in the experimental spectrum is larger than the high-energy maximum.[60]

VIII. Rydberg-Excited Rare Gas Clusters

In the Rydberg-excited rare gas atoms, the excited electron distance from the atom center is larger on average than the interatomic distances between neighboring atoms, which suggests that the interatomic R^* -R potential is determined mainly by the interaction between the ionic core R^+ and neutral R atom. This suggestion is supported by the existence of metastable Rydberg excited rare gas dimers R_2^*, resembling ionic dimers R_2^+.[153-156] The R_2^* potential energy curves, found both experimentally[157-164] and by model[165-166]

and *ab initio*[162,167-171] calculations for low-lying states, demonstrate, however, significantly weaker binding than in the ionic R_2^+. The relatively weak binding between the excited and neutral atoms is attributed mainly to the repulsive forces arising between the excited electron and the electrons of another atom.[172-173] Since the Rydberg-excited R* atom chemical activity is weaker than that of the R^+ ion, the ability of the R* atom to form R_n ($n > 2$) clusters, similar to the R_n^+ clusters, poses a question. According to our knowledge, there is not any experimental evidence about the existence of metastable Rydberg clusters. Experimental studies of R_n^* Rydberg states have been restricted to the problem of the excitation of vdW R_2 dimers[174-176] and R_n clusters[176-179] to autoionizing Rydberg states. For the case of Ar dimers and clusters, the autoionizing states are formed by the excitation of inner-shell electrons, such as 3s[176] or 2p.[179] The 3s → np spectrum of the Ar_3 cluster is found to be similar to that of Ar_2 dimer but with wider resonance lines.[176] This finding cannot be extended automatically to the case of the excitation of the outer 3p electrons, which are affected more strongly by neighboring atoms. The direct study of Rydberg excitations by the measurement of absorption spectra were performed for dimers in Reference 162. Much more is known about the Rydberg excited states in rare gas solids.[16] The information concerning the excitations in solids can be useful for the study of large R_n clusters, but not of the small ones. Any *ab initio* or semiempirical calculations of the Rydberg excited R_n^* ($n > 2$) clusters are unknown to us.

The Rydberg excited R_n^* systems, by analogy with the R_n^+ clusters (Section V) or R_nX systems (Section VII), are made by n closed-shell atoms with one hole which, generally speaking, is moving between atoms. Such systems, as stated in Section IV, can be treated by the semiempirical DIIS method. Since the time of the excited electron motion around the ionic core is much shorter than the time of the hole jump from one atom to another, the excited electron is adiabatically linked to the hole. It follows that applying the DIIS method to the excited clusters we have to consider, instead of the hole motion, the motion of the hole-electron exciton. Neglecting the dipole-dipole interaction, which is expected to be weak in Rydberg-excited

systems, we are left with pairwise interactions which make it possible to use the simplified DIIS Eq. (IV.3). The DIIS method has been applied by us for the calculation of Ar_n^* systems.[180]

In order to calculate the electronic structure of Ar_n^* clusters, one needs as input the Ar_2 and Ar_2^* potentials. The Ar_2 vdW potential, used in the calculation, fits the empirical equilibrium distance and dissociation energy[181] and the *ab initio* potential[182] at small interatomic separations. The Rydberg-excited Ar_2^* potentials are taken from the recent *ab initio* calculation.[169] The Ar_2^* potential curves asymptotic to the $Ar^*(3p^54s^1)$ state are calculated in Reference 169 both without and with spin-orbit (SO) coupling, whereas the Ar_2^* potential curves asymptotic to the $Ar^*(3p^54p^1)$ state are calculated without SO coupling only. As we restrict ourself to the Rydberg excited atomic states $3p^54s^1$ and $3p^54p^1$, we shall denote further these states simply by the excited electron orbitals 4s and 4p.

According to the results of the DIIS calculation presented in Table 7, the 4s excited atoms in the states $^1\Sigma_u^+$ and $^3\Sigma_u^+$ without SO coupling and $C(0_u^+)$ with SO coupling really form metastable Ar_3^* clusters. All of these clusters have a symmetrical linear geometry, like the Ar_3^+ clusters (Section IV), with the Ar-Ar distances slightly larger than in the corresponding states of the Ar_2^* dimer. However, in contrast to the Ar_3^+ cluster with a dissociation energy D_e of 0.2 eV, the dissociation energies of these metastable Ar_3^* clusters are small, ranging in the interval 0.01-0.04 eV. In the state asymptotic to $Ar^*\ ^1P_1(4s)$, in addition to the collinear metastable cluster, a less-stable cluster with the geometry of an equilateral triangle is formed. The Rydberg 4s excited atom in orther states with SO coupling ($^3P_1$ and $^3P_2$) do not form any metastable clusters, in spite of the fact that they form relatively strongly-bound metastable dimers (Table 7). The Ar_3^* clusters formed by Ar*(4s) atoms attract more atoms but with so small dissociation energy (0.001-0.002 eV) that the very existence of the metastable Ar_n^* ($n > 3$) clusters asymptotic to Ar(4s) is under question.

The behavior of the Ar* atom excited to the Rydberg 4p state shows much more similarity to the behavior of the Ar^+ ion, which is easily explained by the more diffuse character of the 4p orbital compared to the 4s. According to

the DIIS calculation, the dissociation energy D_e of the metastable Ar_3^* cluster in the state asymptotic to Ar* $^3D_e(4p)$ is 0.23 eV (Table 7) and exceeds even the Ar_3^+ dissociation energy of 0.2 eV (Section V). This Ar_3^* cluster attracts more Ar atoms, forming larger metastable Ar_n^* clusters, like in the case of ionic clusters.

Calculating the energy of the Rydberg excited Ar_n^* clusters in the geometry of the ground state (vdW) Ar_n clusters, we can determine the Ar_n vertical excitation energies (for the vdW clusters geometry see Section II). This energy is determined as the difference between the energies of the excited and ground states in the same geometry. According to the results of the calculation, the energy of the cluster dissociation to separated atoms in the Rydberg excited states is on the same order as in the ground states, so that both of these dissociation energies are of importance for the determination of the excitation energy. The dissociation energy of the ground state (vdW) clusters Ar_n increases monotonically with n (Section II), coming up to 0.49 eV for the "magic" Ar_{13} cluster. The dependence of the excited states dissociation energy on n is more varied. In the states asymptotic to the Ar*(4s) states ^1P and ^3P (without SO coupling) and $^1P_1$ (with SO coupling), the energy of the excited states decreases monotonically with the number of atoms n, almost at the same rate as the vdW clusters, which makes the excitation energy dependence on n very weak. For example, in the case of the cluster excited state asymptotic to the atomic $^1P_1$ state, the excitation energy decreases slightly with n, up to n = 4-6, and increases for n > 6, but slowly so that the Ar_{13} excitation energy is only 0.14 eV higher than the atomic Ar excitation energy. The situation is different in the triplet states with SO coupling asymptotic to the $Ar^*(4s)$ $^3P_1$ and $^3P_2$ atomic states, where the variations in the excitation state energy dependence on n are small. As a result, the excitation energy is increasing monotonically with the number of atoms n, due to the decrease in the energy of the vdW clusters. For example, the Ar_{13} excitation energies to the cluster states asymptotic to the atomic $^3P_1$ and $^3P_2$ states are larger than the corresponding Ar atomic excitation energies by 0.34 eV and 0.29 eV, respectively. Unfortunately, there are not any experimental data on the vdW Ar_n clusters $3p \rightarrow 4s$ excitations.

The increase, if weak, of the vdW cluster excitation energy with the cluster size is in contrast to the behavior of the cluster ionization potential. Due to the polarization energy and hole delocalization, the energy of the ionic cluster (in the geometry of the vdW cluster) decreases with cluster size much more strongly than the vdW cluster energy, causing relatively strong decrease in the ionization potential.[183] For example, we have found the ionization potential of Ar_{13} to equal 14.46 eV, smaller by 1.41 eV than the atom Ar ionization potential (15.51 eV). It is interesting to note that in the lowest excited Ar_{13}^* states, the excited electron is delocalized between the 12 outer Ar atoms, leaving the central atom almost unexcited. In contrast to this, in the ionic Ar_{13}^+ cluster (in the geometry of the vdW Ar_{13} cluster), the charge is concentrated on the central atom.

IX. Concluding Remarks

The rare gas atom R becomes chemically active when it looses an outer shell electron. In clusters, the electron removed from the atomic shell is either eliminated from the cluster or left inside it. In the first case, an ionic cluster is formed, for example R_n^+. The second case can be realized in any cluster by Rydberg excitation ($R_{n-1}R^+e^-$ complex) and in a halogen X-containing cluster excited by R → X electron transfer ($R_{n-1}R^+X^-$ complex). Due to the chemical activity of the R^+ ion or ionic core, R^+-R valence attraction arises which leads to the formation of a strongly-bound R_2^+ or R_n^+ ($n > 2$) fragment. The ionic fragment attracts other atoms by polarization forces. These two main interactions, namely the valence binding resulting from the positive charge delocalization and the polarization attraction, are taken into account by our semiempirical diatomics-in-ionic-systems (DIIS) method, which has been used to treat the rare gas clusters and solids containing charged atoms.

The structure and properties of systems formed by two rare gas atoms, such as R_2^+, R_2^* and $R_2^+X^-$, are well known. We have less reliable knowledge, unfortunately, about the systems R_n^+, R_n^* and $R_n^+X^-$ with three or more rare gas atoms. From experimental and theoretical studies, it is known that the ionic

clusters R_n^+, exist, but the structure of these clusters is still not unequivocally clear. However, most calculations, including our DIIS calculation, have shown the smallest ionic clusters, R_3^+, to be of a symmetrical linear geometry. In other calculations the R_3^+ geometry is found to be asymmetrical. The experimental evidences concerning the R_3^+ structure are also contradictory. The explanation of some ambiguity in the R_3^+ structure lies, probably, in the features of its potential energy surfaces which are almost flat over wide intervals of interatomic distances, so that the thermal motion easily shifts the cluster geometry far away from the equilibrium configuration. The same holds to an even in a greater extent for the R_n^+ clusters with more than three atoms, which have several isomers with almost the same energy. The situation is similar in the case of clusters with $R \rightarrow X$ electron transfer, such as $R_{n-2}R_2^+Cl^-$ clusters. In the Rydberg excited clusters, the valence and polarization forces are less strong than in the ionic clusters, at least the lowest $np^6(n+1)s^1$ excited state. According to our calculations, the very existence of such excited R_n^* ($n > 2$) clusters is under question. In higher excited states the R^*-R interactions look more like the R^+-R interactions, so that more similarity is expected in the structure of highly-excited R_n^* and ionic R_n^+ clusters.

In ionic clusters R_n^+ with more than four atoms, the charge is concentrated on a smaller number of atoms, which form an ionic core so that the structure of a cluster is $R_{n-k}R_k^+$. The size and geometry of this ionic core depends, most likely, on the cluster size n. The results of both theoretical and experimental studies concerning the size and the geometry of the ionic cores are contradictory. According to our calculation, in the Xe_n^+ clusters the ionic core has the configuration of a fully symmetrical equilateral Xe_4^+ pyramid. In the rare gas solids doped by halogen atoms in the excited states with $R \rightarrow X$ electron transfer, the $R_2^+Cl^-$ molecule plays the role of the ionic core.

Acknowledgments

This research was supported by the National Science Foundation under Grant CHE-9196214 and the Office of Naval Research.

References

1. C. Kittel, *Introduction to Solid State Physics* (Wiley, New York, 1976), p. 15.
2. M. R. Hoare, *Adv. Chem. Phys.* **40**, 49 (1979).
3. T. J. Beck, J. D. Doll and D. Freeman, *J. Chem. Phys.* **90**, 5651 (1990).
4. D. J. Wales and R. S. Berry, *J. Chem. Phys.* **92**, 4283 (1990).
5. C. Y. Ng, Y. T. Lee and J. A. Barker, *J. Chem. Phys.* **61**, 1996 (1974).
6. J. M. Parson, P. E. Siska and Y. T. Lee, *J. Chem. Phys.* **56**, 1511 (1972).
7. P. J. Hay and T. H. Dunning, Jr., *J. Chem. Phys.* **66**, 1306 (1977).
8. I. Last and T. F. George, *J. Chem. Phys.* **87**, 1183 (1987).
9. R. J. LeRoy and J. M. Hutson, *J. Chem. Phys.* **86**, 837 (1987).
10. P. A. Christiansen, K. S. Pitzer, Y. S. Lee, J. H. Yates, W. C. Ermler and N. W. Winter, *J. Chem. Phys.* **75**, 5410 (1981).
11. P. M. Dehmer and J. L. Dehmer, *J. Chem. Phys.* **76**, 125 (1978).
12. D. L. Turner and D. C. Conway, *J. Chem. Phys.* **71**, 1899 (1979).
13. W. R. Wadt, *Appl. Phys. Lett.* **38**, 1030 (1981).
14. I. Last and T. F. George, *J. Chem. Phys.* **93**, 8925 (1990).
15. K. Norwood, J.-H. Guo and C. Y. Ng, *J. Chem Phys.* **90**, 2995 (1989).
16. M. Schwentner, E.-E. Koch and J. Jortner, *Electronic Excitations in Condensed Rare Gases. Springer Tracts in Modern Physics*, Volume **107** (Springer-Verlag, Berlin-Heidelberg, 1985), Sec. 3.
17. W. Miehle, O. Kandler, T. Leisner and O. Echt, *J. Chem. Phys.* **91**, 5940 (1989).
18. W. R. Wadt, *J. Chem. Phys.* **68**, 402 (1978).
19. D. C. Lorents, *Physica C* **82**, 19 (1976).
20. K. P. Killeen and J. G. Eden, *J. Chem. Phys.* **84**, 6048 (1986).
21. V. Sidis, *J. Phys. B* **5**, 1517 (1972).
22. P. Rosmus, *Theor. Chim. Acta* **51**, 359 (1979).
23. K. B. Laughlin, G. A. Blake, R. C. Cohen, D. C. Hovde and R. J. Saykally, *Phys. Rev. Lett.* **58**, 996 (1987).
24. G. A. Gallup and J. Macek, *J. Phys. B* **10**, 1601 (1977).
25. D. K. Bohme, G. I Mackay and H. I. Shift, *J. Chem. Phys.* **73**, 4976 (1980).

26. R. Klein and P. Rosmus, *Z. Naturforsch.* **39a**, 349 (1984).

27. S. A. Rogers, C. R. Brazier and P. F. Bernath, *J. Chem. Phys.* **87**, 159 (1987).

28. E. Clementi and C. Roetti, *At. Data Nucl. Data Tables* **14**, 177 (1974).

29. M. Waldman and R. Gordon, *J. Chem. Phys.* **71**, 1325 (1979).

30. J. A. Northby, *J. Chem. Phys.* **87**, 6166 (1987).

31. D. Eichenauer and R. J. LeRoy, *Phys. Rev. Lett.* **57**, 2920 (1986).

32. D. D. Evard, J. I. Cline and K. C. Janda, *J. Chem. Phys.* **88**, 5433 (1988).

33. S. R. Hair, J. I. Cline, C. R. Bieler and K. C. Janda, *J. Chem. Phys.* **90**, 2935 (1989).

34. A. Penner, A. Amirav, J. Jortner and A. Nitzan, *J. Chem. Phys.* **93**, 147 (1990)

35. E. Shalev, N. Ben-Horin, U. Even and J. Jortner, *J. Chem. Phys.* **95**, 3147 (1991).

36. B. J. Howard and A. S. Pine, *Chem. Phys. Lett.* **122**, 1 (1985).

37. G. T. Frazer and A. S. Pine, *J. Chem. Phys.* **85**, 2502 (1986).

38. T. D. Klots, R. S. Ruoff, C. Chuang, T. Emilsson and H. S. Gutowski, *J. Chem. Phys.* **87**, 4383 (1987).

39. I. Last and T. F. George, *J. Chem. Phys.* **89**, 3071 (1988).

40. D. D. Evard, F. Thommen, J. I. Cline and K. C. Janda, *J. Phys. Chem.* **91**, 2508 (1987).

41. F. Salama and J. Fournier, *Chem. Phys. Lett.* **120**, 35 (1985).

42. E. Boursay, *J. Chem. Phys.* **62**, 3353 (1975).

43. R. McWeeny and B. T. Sutcliffe, *Methods of Molecular Quantum Mechanics* (Academic, New York, 1969), Section 7.

44. A. Sur, A. K. Hui and J. Tellinghuisen, *J. Mol. Spectrosc.* **74**, 465 (1979).

45. P. J. Hay and T. H. Dunning, Jr., *J. Chem. Phys.* **69**, 2209 (1978).

46. G. Malm, H. Selig, J. Jortner and S. A. Rice, *Chem. Rev.* **65**, 199 (1965).

47. W. F. Howard, Jr. and L. Andrews, *J. Amer. Chem Soc.* **96**, 7864 (1974).

48. B. W. Yates, K. H. Tan, G. M. Bancroft and L. L. Coatsworth, *J. Chem. Phys.* **84**, 3603 (1986).

49. I. Last and T. F. George, *J. Chem. Phys.* **86**, 3787 (1987).

50. J. R. Platt, *J. Chem. Phys.* **18**, 932 (1950).

51. H.-Y. Kim and M. W. Cole, *J. Chem. Phys.* **90**, 6055 (1989).

52. A. Wallqvist, D. Thirumalai and B. J. Berne, *J. Chem. Phys.* **86**, 6404 (1987).

53. N. Ben Horin, U. Even and J. Jortner, *J. Chem. Phys.* **91**, 331 (1989).

54. W. E. Baylis, *J. Chem. Phys.* **51**, 2665 (1969).

55. P. E. Siska, *J. Chem. Phys.* **71**, 3942 (1979).

56. K. Haug and H. Metiu, *J. Chem. Phys.* **95**, 5670 (1991).

57. I. Last and T. F. George, *Chem. Phys. Lett.* **183**, 547 (1991).

58. J. Jortner, S. Leutwyler and Z. Berkovitch-Yellin, *J. Chem. Phys.* **78**, 309 (1983).

59. M. E. Fajardo and V. A. Apkarian, *J. Chem. Phys.* **85**, 5660 (1986).

60. I. Last, T. F. George, M. E. Fajardo and V. A. Apkarian, *J. Chem. Phys.* **87**, 5917 (1987).

61. I. Ts. Lyast, *J. Struct. Chem.* **16**, 355 (1975).

62. J. C. Tully, *Adv. Chem. Phys.* **42**, 63 (1980).

63. I. Last, *Chem. Phys.* **55**, 237 (1981).

64. M. Lezius. P. Scheier, A. Stamatovic and T. D. Märk, *J. Chem. Phys.* **91**, 3240 (1989).

65. N. G. Gotts, P. G. Lethbridge and A. J. Stace, *J. Chem. Phys.* **96**, 408 (1992).

66. H. H. Michels, R. H. Hobbs and L. A. Wright, *Appl. Phys. Lett.* **35**, 153 (1979).

67. M. Rosi and C. W. Bauschilcher Jr., *Chem. Phys. Lett.* **159**, 479 (1989).

68. O. K. Kabbaj, M.-B. Lepetit and J.-P. Mairieu, *Chem. Phys. Lett.* **172**, 483 (1990).

69. H.-U. Bohmer and S. D. Peyerimhoff, *Z. Phys. D* **5** 195 (1986).

70. J. Hesslich and P. J. Kuntz, *Z. Phys. D* **2**, 251 (1990).

71. P. J. Kuntz and J. Valldorf, *Z. Phys. D* **8**, 195 (1988).

72. F. X. Gadea and M. Amarouch *Chem. Phys.* **140**, 385 (1990).

73. M. Amarouch, G. Durand and J. P. Malrieu, *J. Chem. Phys.* **88**, 1010 (1988).

74. M. T. Bowers, W. E. Palke, K. Robins, C. Roehl and S. Walsh, *Chem. Phys. Lett.* **180**, 235 (1991).

75. K. Hiraoka and T. Mori, *J. Chem. Phys.* **90**, 7143 (1989).

76. J. T. Snodgrass, C. M. Roehl and M. Bowers, *Chem. Phys. Lett.* **159**, 10 (1989).

77. N. E. Levinger, D. Ray, M. L. Alexander and W. C. Lineberger, *J. Chem. Phys.* **89**, 5654 (1988).

78. N. E. Levinger, D. Ray, K. K. Murray, A.S. Mullin, C. P. Schulz and W. C. Lineberger, *J. Chem. Phys.* **89**, 71 (1988).

79. C. R. Albertoni, R. Kuhn, H. W. Sarkas and A. W. Castleman, Jr., *J. Chem. Phys.* **87**, 5043 (1987).

80. Z. Y. Chen, C. R. Albertoni, M. Hasegawa, R. Kuhn and A. W. Castleman, Jr., *J. Chem. Phys.* **91**, 4019 (1989).

81. T. Nagata, J. Kirokawa, T. Ikegami, T. Kondow and S. Iwata, *Chem. Phys. Lett.* **171**, 433 (1990).

82. C. A. Woodward, J. E. Upham, A. J. Stace and J. N. Murrell, *J. Chem. Phys.* **91**, 7612 (1989).

83. M. J. Deluca and M. A. Johnson, *Chem. Phys. Lett.* **162**, 445 (1989).

84. N. G. Gotts, R. Hallett, J. A. Smith and A. J. Stace, *Chem. Phys. Lett.* **181**, 491 (1991).

85. P. L. Patterson, *J. Chem. Phys.* **48**, 3625 (1968).

86. F. C. Fehsenfeld, T. J. Brown and D. L. Albritton, *Proc. 31st Gaseous Electronic Conference* (Buffalo, New York, 1978); *Bull. Am. Phys. Soc.* **24**, 124 (1979).

87. H. Helm, *Phys. Rev. A* **14**, 680 (1976).

88. H. Haberland, B. von Issendorf, T. Kolar, H. Kornmeier, C. Ludewight and A. Risch, *Phys. Rev. Lett.* **67**, 3290 (1991).

89. P. M. Dehmer and S. T. Pratt, *J. Chem. Phys.* **76**, 843 (1982).

90. I. A. Harris, R. S. Kidwell and J. A. Northby, *Phys. Rev. Lett.* **53**, 2390 (1984).

91. M. Haberland, *Surf. Sci.* **156**, 305 (1985).

92. J. J. Saenz, J. M. Soler and N. Garcia, *Surf. Sci.* **156**, 120 (1985).

93. H.-U. Bohmer and S. D. Peyerimhoff, *Z. Phys. D* **11**, 239 (1989).

94. A. J. Stace, *J. Chem. Phys.* **85**, 5774 (1986).

95. P. G. Lethbridge and A. J. Stace, *J. Chem. Phys.* **89**, 4062 (1988).

96. F. X. Gadea and J. Durup, *Chem. Phys. Lett.* **181**, 378 (1991).

97. F. Carnovale, J. B. Peel and R. G. Rothwell, *J. Chem. Phys.* **95**, 1473 (1991).

98. M. Umhera, *Proceedings of Vacuum Ultraviolet Radiation Physics, VUV* **2**, 279 (1983).

99. H. Buchenau, E. L. Knath, J. Northby, J. P. Toennies and C. Winkler, *J. Chem. Phys.* **92**, 6875 (1990).

100. K. Balasubramanian, *J. Chem. Phys.* **93**, 8403 (1990).

101. P. W. Stephens and J. G. King, *Phys. Rev. Lett.* **51**, 1538 (1983).

102. S. Wei, Z. Shi and A. W. Castleman, Jr., *J. Chem. Phys.* **94**, 8604 (1991).

103. A. Ding and J. Hessling, *Chem. Phys. Lett.* **94**, 54 (1983).

104. F. Carnovale, J. B. Peel, R. G. Rothwell, J. Valldorf and P. J. Kuntz, *J. Chem. Phys.* **90**, 1452 (1989).

105. A. J. Stace, C. A. Woodward and B. J. Whitaker, *Chem. Phys. Lett.* **184**, 113 (1991).

106. C. A. Woodward and A. J. Stace, *J. Chem. Phys.* **94**, 4234 (1991).

107. R. Casero and J. M. Soler, *J. Chem. Phys.* **95**, 2927 (1991).

108. M. Foltin and T. D. Märk, *Chem. Phys. Lett.* **180**, 317 (1991).

109. O. Echt, K. Sattler and E. Recknagel, *Phys. Rev. Lett.* **47**, 1121 (1981).

110. S. Chapman and R. K. Preston, *J. Chem. Phys.* **60**, 650 (1974).

111. M. Baer and H. Nakamura, *J. Chem. Phys.* **87**, 4651 (1987).

112. C. Rebrion, B. R. Rowe and J. B. Marquette, *J. Chem. Phys.* **91**, 6142 (1987).

113. P. J. Kuntz and A. C. Roach, *J. Chem. Soc. Faraday Trans. II* **68**, 259 (1972).

114. M. Bogey, H. Bolvin, C. Demuynck, J. L. Destombes and B. P. K. Eijck, *J. Chem. Phys.* **88**, 4120 (1988).

115. C. E. Dykstra, *J. Mol. Struct.* **103**, 131 (1983).

116. E. D. Simandiras, J. F. Gaw and N. C. Handy, *Chem. Phys. Lett.* **141**, 166 (1987).

117. M. Okumare, L. I. Yeh and Y. T. Lee, *J. Chem. Phys.* **88**, 79 (1988).

118. Y. K. Bae, *Chem. Phys. Lett.* **180**, 179 (1991).

119. R. L. Matcha and M. B. Milleur, *J. Chem. Phys.* **68**, 4748 (1978); **69**, 3016 (1978).

120. E. J. Bieske, A. M. Soliva, A. Friedmann and J. P. Maier, *J. Chem. Phys.* **96**, 28 (1992).

121. J. Jortner, U. Even, S. Leutwyler and Z. Berkovitch-Yelin, *J. Chem. Phys.* **78**, 309 (1984).

122. T. Troxler, R. Knochenmuss and S. Leutwyler, *Chem. Phys. Lett.* **159**, 554 (1989).

123. W. R. Peifer, M. T. Coolbaugh and J. F. Garvey, *J. Phys. Chem.* **93**, 4700 (1989).

124. W. R. Peifer and J. F. Garvey, *J. Phys. Chem.* **93**, 5906 (1989).

125. H. P. Kaukonen, U. Landman and C. L. Cleveland, *J. Chem. Phys.* **95**, 4997 (1991).

126. J. Geersten and G. E. Scuseria, *J. Chem. Phys.* **90**, 6486 (1989).

127. M. E. Rosenkrantz, *Chem. Phys. Lett.* **173**, 378 (1990).

128. H. Kunttu, J. Seetula, M. Rasanen and V. A. Apkarian (to be published).

129. S. K. Searles and G. A. Hart, *Appl. Phys. Lett.* **27**, 243 (1975).

130. J. A. Mangano and J. H. Jacob, *Appl. Phys. Lett.* **27**, 495 (1975).

131. C. A. Brau and J. J. Ewing, *J. Chem. Phys.* **63**, 4640 (1975).

132. V. S. Dubov, L. I. Gudzenko, L. V.Gurvich and S. I. Iakovlenko, *Chem. Phys. Lett.* **53**, 170 (1978).

133. F. K. Tittel, W. L. Wilson, R. E. Stickel, G. Marowski and W. E. Ernst, *Appl. Phys. Lett.* **36**, 405 (1980).

134. J. Tellinghuisen and M. R. McKeeven, *Chem. Phys. Lett.* **72**, 94 (1980).

135. V. S. Dubov, Y. E. Lapsker, A. N. Samoilova and L. V. Gurvich, *Chem. Phys. Lett.* **83**, 518 (1981).

136. A. W. McCown and J. C. Eden, *J. Chem. Phys.* **81**, 2933 (1984).

137. B. S. Ault and L. Andrews, *J. Chem. Phys.* **65**, 4192 (1976).

138. H. Jara, J. Pummer, H. Egger and C. K. Rhodes, *Phys. Rev. B* **30**, 1 (1984).

139. M. E. Fajardo and V. A. Apkarian, *Chem. Phys. Lett.* **134**, 51 (1987).

140. L. Wiedman, M. E. Fajardo and V. A. Apkarian, *Chem. Phys. Lett.* **134**, 35 (1987).

141. M. E. Fajardo and V. A. Apkarian, *J. Chem. Phys.* **89**, 4102 (1988).

142. H. Kunttu, E. Sekreta and V. A. Apkarian, *J. Chem. Phys.* **94**, 7819 (1991).

143. N. Schwentner, M. E. Fajardo and V. A. Apkarian, *Chem. Phys. Lett.* **154**, 237 (1989).

144. W. R. Wadt and P. J. Hay, *J. Chem. Phys.* **68**, 3850 (1978).

145. W. J. Stevens and M. Krauss, *Appl. Phys. Lett.* **41**, 301 (1982).

146. D. L. Huestis and N. E. Schlotter, *J. Chem. Phys.* **69**, 3100 (1978).

147. D. L. Huestis, G. Marowski and F. K. Tittel, in *Excimer Lasers - 1983*, ed. C. K. Rhodes, H. Egger and H. Pummer (American Institute of Physics, (New York, 1983), pp. 238-248.

148. J. G. McCaffrey, H. Kunz and N. Schwentner, *J. Chem. Phys.* **96**, 2825 (1992).

149. R. L. Robinson, Dz-H. Gwo, D. Ray and R. J. Saykally, *J. Chem. Phys.* **86**, 5211 (1987).

150. J. M. Hutson, J. A. Beswik and N. Halberstadt, *J. Chem. Phys.* **90**, 1337 (1989).

151. H. Kunz, J. G. McCaffrey, M. Chergui, R. Schriever, O. Unal, V. Stepanenko and N. Schwentner, *J. Chem. Phys.* **95**, 1466 (1991).

152. K.-S. Lam and T. F. George, *J. Chem. Phys.* **90**, 1048 (1989).

153. P. E. LaRocque, R. H. Lipson, P. R. Herman and B. P. Stoicheff, *J. Chem. Phys.* **84**, 6627 (1986).

154. T. Moller, J. Stapelfeldt, M. Beland and G. Zimmerer, *Chem. Phys. Lett.* **117**, 301 (1985).

155. P. M. Dehmer, S. T. Pratt and J. L. Dehmer, *J. Chem. Phys.* **85**, 13 (1986).

156. P. M. Dehmer, S. T. Pratt and J. L. Dehmer, *J. Phys. Chem.* **91**, 2593 (1987).

157. K. T. Gillen, R. P. Saxon, D. C. Lorents, G. E. Ice and R. E. Olson, *J. Chem. Phys.* **64**, 1925 (1976).

158. Y. Tanaka, W. C. Walker and Y. Tanaka, *J. Chem. Phys.* **70**, 380 (1979).

159. D. E. Freeman, K. Yoshino and Y. Tanaka, *J. Chem. Phys.* **71**, 1780 (1979).

160. Y. Matsura and K. Fukuda, *J. Phys. Soc. Jpn.* **50**, 933 (1981).

161. P. R. Herman, P. E. LaRocque and B. P. Stoicheff, *J. Chem. Phys.* **89**, 4535 (1988).

162. M. C. Castex, M. Morlais, F. Spiegelmann and J. P. Malrieu, *J. Chem. Phys.* **75**, 5006 (1981).

163. K. Barzen, P. Wollenweber and H. Schmoranzer, *Chem. Phys. Lett.* **142**, 79 (1987).

164. S. B. Kim, C. M. Herring and J. G. Eden, *J. Chem. Phys.* **96**, 1016 (1992).

165. O. Vallee, J. Glasser, P. Ranson and J. Chapelle, *J. Chem. Phys.* **69**, 5091 (1978).

166. O. Vallee, N. T. Minch and J. Chapelle, *J. Chem. Phys.* **73**, 2784 (1980).

167. J. H. Yates, W. C. Ermler, N. W. Winter, P. A. Christiansen, Y. S. Lee and K. S. Pitzer, *J. Chem. Phys.* **79**, 6145 (1983).

168. F. Spiegelmann and F. X. Gadea, *J. Phys. (Paris)* **45**, 1003 (1984).

169. Y. Mizukami and H. Nakatsuji, *J. Chem. Phys.* **92**, 6084 (1990).

170. Y. Mizukami and H. Nakatsuji, *J. Mol. Struct. (Theochem.)* **234**, 469 (1991).

171. E. Audouard and F. Spiegelmann, *J. Chem. Phys.* **94**, 6102 (1991).

172. R. S. Mulliken, *J. Chem. Phys.* **52**, 5170 (1970).

173. K. Haug and H. Metiu, *J. Chem. Phys.* **95**, 5670 (1991).

174. C. Y. Ng, D. J. Trevor, B. H. Mahan and Y. T. Lee, *J. Chem. Phys.* **66**, 446 (1977).

175. P. M. Dehmer and E. D. Poliakoff, *Chem. Phys. Lett.* **77**, 326 (1981).

176. M. G. White and J. R. Grover, *J. Chem. Phys.* **79**, 4124 (1983).

177. C. Y. Ng, *Adv. Chem. Phys.* **52**, 263 (1983).

178. W. Kamke, J. de Vries, J. Krauss, E. Kaiser, B. Kamke and I. V. Hertel, *Z. Phys. D* **14**, 339 (1989).

179. E. Ruhl, H. W. Jochims, C. Schmale, E. Biller, A. P. Hitchcock and H. Baumgartel, *Chem. Phys. Lett.* **178**, 558 (1991).

180. I. Last and T. F. George (in preparation).

181. R. A. Aziz and M. J. Slaman, *Mol. Phys.* **58**, 679 (1986).

182. A. D. McLean, B. Liu and J. A. Barker, *J. Chem. Phys.* **89**, 6339 (1988).

183. A. M. Findley, S. Bernstoff and G. L. Findley, *Chem. Phys. Lett.* **131**, 349 (1986).

Table 1. Atomic radii r (in Å), ionization potentials I (in eV) and polarizabilities α (in $Å^3$).

Atom	r	I	α
He	1.33	24.58	0.205
Ne	1.60	21.56	0.395
Ar	1.92	15.755	1.640
Kr	1.98	14.00	2.487
Xe	2.18	12.13	4.017

Table 2. Experimental interatomic equilibrium distances R (in Å) and dissociation energies D_0 (in eV) of van der Waals R_2 molecules. (These are taken from Reference 29.)

Molecule:	He_2	Ne_2	Ar_2	Kr_2	Xe_2
R	2.96	3.11	3.76	4.01	4.37
D_0	0.0024	0.0095	0.031	0.052	0.085

Table 3. Results of model calculations for the equilibrium distances between neighboring atoms R (in Å), dissociation energies D_e and atom detachment energies D_A (in eV) of van der Walls Ar_n clusters.

n:	2	3	4	6	9	13	14
R	3.75	3.75	3.74	3.725	3.72	3.71	3.71
D_e	0.012	0.036	0.072	0.153	0.265	0.489	0.544
D_A	0.012	0.024	0.036	0.051	0.065	0.070	0.055

Table 4. Structure of the ionic clusters Ar_n^+ and ionic molecule Ar_2^+. The distances (R) are in Å, and the ground-state and dissociation energies E and D_e respectively, in eV. (These are taken from Reference 14.)

N	Ar_n^+	Structure [1]	R [2]	R [3]	q [4]	E	Dissociation Products	D_e
I	Ar_2^+		2.48			-1.240	$Ar^+ + Ar$	**1.240**
II	Ar_3^+	linear	2.59			-1.443	$Ar_2^+ + Ar$	**0.203**
III	Ar_4^+	$(Ar_3^+)_z(Ar)_{xz}$	2.59	3.68	0.002	-1.490	$Ar_3^+ + Ar$	**0.047**
IV	Ar_4^+	regular pyramid	2.836			-1.480	$Ar_2^+ + 2Ar$	**0.240**
V	Ar_4^+	linear	2.59	3.3	0.01	-1.474	$Ar_3^+ + Ar$	0.031
VI	Ar_5^+	$(Ar_3^+)_z(Ar_2)_{xy}$	2.59	3.68	0	-1.540	$(Ar_4^+)_{III} + Ar$	**0.050**
VII	Ar_5^+	$(Ar_3^+)_z(Ar_2)_{xz}$	2.59	3.61	0.002	-1.540	$(Ar_4^+)_{III} + Ar$	**0.050**
VIII	Ar_5^+	$(Ar_3^+)_z(Ar_2)_{xz}$	2.59	3.68	0.003	-1.537	$(Ar_4^+)_{III} + Ar$	**0.047**
IX	Ar_6^+	$(Ar_3^+)_2(Ar_2)_{xy}(Ar)_x$	2.59	3.61	0.001	-1.601	$(Ar_5^+)_{VI} + Ar$	**0.061**

[1] The subscripts z, xz, etc. denote the location along an axis or in a plane (see Figure 1).

[2] Distance between adjacent charged atoms.

[3] Distance from a neutral or weakly-charged atom to the nearest charged atom.

[4] Common charge of all weakly-charged atoms.

Table 5. Structures of the ionic clusters Xe_n^+ and ionic molecule Xe_2^+. (See Table 4 for the footnotes.)

N	Xe_n^+	Structure [1]	R [2]	R [3]	q [4]	E	Dissociation Products	D_e
I	Xe_2^+		3.22			-1.080	$Xe^+ + Xe$	1.08
II	Xe_3^+	linear	3.383			-1.277	$Xe_2^+ + Xe$	0.197
III	Xe_4^+	regular pyramid	3.646			-1.480	$Xe_2^+ + 2Xe$	0.40
IV	Xe_4^+	$(Xe_3^+)_z(Xe)_{xz}$	3.384	4.19	0.014	-1.356	$Xe_3^+ + Xe$	0.079
V	Xe_4^+	linear	3.315	3.65	0.184	-1.346	$Xe_3^+ + Xe$	0.069
VI	Xe_5^+	$(Xe_4^+)_{III}(Xe)_{xz}$	3.646	4.40	0.001	-1.568	$Xe_4^+ + Xe$	0.088
VII	Xe_5^+	$(Xe_3^+)_z(Xe_2)_{xz}$	3.383	4.24	0.005	-1.439	$Xe_3^+Xe + Xe$	0.083
VIII	Xe_6^+	$(Xe_4^+)_{III}Xe_2$	3.644	4.40	0	-1.637	$Xe_4^+Xe + Xe$	0.069
IX	Xe_6^+	$(Xe_3^+)_z(Xe_3)_{xz}$	3.375	4.20	0.021	-1.547	$Xe_3^+Xe_2 + Xe$	0.108

Table 6. Structures of the ionic clusters $Ar_k(ArH)^+$ and ionic molecule $(ArH)^+$. The distances (R) are in Å, the energies (E) in eV and the dipole moments (μ) in Debyes. (These are taken from Reference 14.)

$Ar_k(ArH)^+$	q_H [1]	R_{Ar-H} [2]		R_{Ar-Ar} [2]		μ	E	Ar Detachment
$(ArH)^+$	0.569					2.78	-4.055	
$Ar(ArH)^+$	0.579	2.81		3.70		5.98	-4.218	0.163
$Ar_2(ArH)^+$	0.591	2.79		3.81		6.32	-4.395	0.177
$Ar_3(ArH)^+$	0.601	2.79		3.72		6.23	-4.586	0.191
$Ar_4(ArH)^+$	0.609	2.84		3.57		4.94	-4.760	0.174
$Ar_6(ArH)^+$	0.614	2.84	3.17	3.87	3.38	3.33	-4.947	0.094

[1] Charge of the H atom in $(ArH)^+$

[2] R_{Ar-H} and R_{Ar-Ar} are the distances from the neutral atom to H and Ar of $(ArH)^+$, respectively. For $Ar_6(ArH)^+$ there are two different Ar-H and Ar-Ar distances.

Table 7. Structure of the Rydberg excited Ar_2^* dimers and linear symmetrical Ar_3^* clusters in metastable configurations. The dissociation energies D_e of $Ar_2^* \rightarrow Ar^* + Ar$ and $Ar_3^* \rightarrow Ar_2^* + Ar$ atom detachment are in eV, and the equilibrium distances R_e are in Å. The distribution of the excitation among the Ar_3^* atoms is presented by q_i, i = 2 being the central atom. (These are taken from Reference 180.)

		Without SO			With SO		
Ar^*	State excitation energy	$^3P(4s)$ 11.58	$^1P(4s)$ 11.88	$^1D(4p)$ 13.09	$^3P_2(4s)$ 11.52	$^3P_1(4s)$ 11.61	$^1F_1(4s)$ 11.87
Ar_2^*	State	$^3\Sigma_u^+$	$^1\Sigma_u^+$	$^1\Pi_g$	$A(0_u^-)$	$B(0_u^+)$	$C(0_u^+)$
	R_e	2.48	2.48	2.46	2.52	2.47	3.60
	D_e	0.49	0.56	0.79	0.42	0.31	0.055
Ar_3^*	R_e	2.59	2.58	2.515	-	-	3.63
	D_e	0.008	0.042	0.232	-	-	0.028
	q_1	0.16	0.15	0.09	-	-	0.31
	q_2	0.68	0.70	0.82	-	-	0.38
	q_3	0.16	0.15	0.09	-	-	0.31

Figure Captions

1. Ar_3^+ and Ar_4^+ geometries. The Roman numerals indicate the clusters (the same as in Table 4). The numbers without signs are distances in Å, and the numbers with the + sign are the atomic charges. (This figure is taken from Reference 14.)

2. Xe_3^+ and Xe_4^+ geometries. For notations see Figure 1. (This figure is taken from Reference 14.).

3. Geometries of the quasistable XeHCl clusters in the states with electron transfer. The numbers stand for interatomic distances in Å and atomic charges. The energies (relative to the van der Waals cluster) of the quasistable ground-state isomer 1i and the excited-states isomers 3i and 4i are 4.24 eV, 7.34 eV and 8.43 eV, respectively. (This figure is taken from Reference 39.)

4. Energy spectrum of the $Xe_{12}Cl$ cage excitation from the ground to excited states with Xe → Cl electron transfer. The temperature is 10 K. (This figure is taken from Reference 60.)

Figure 1

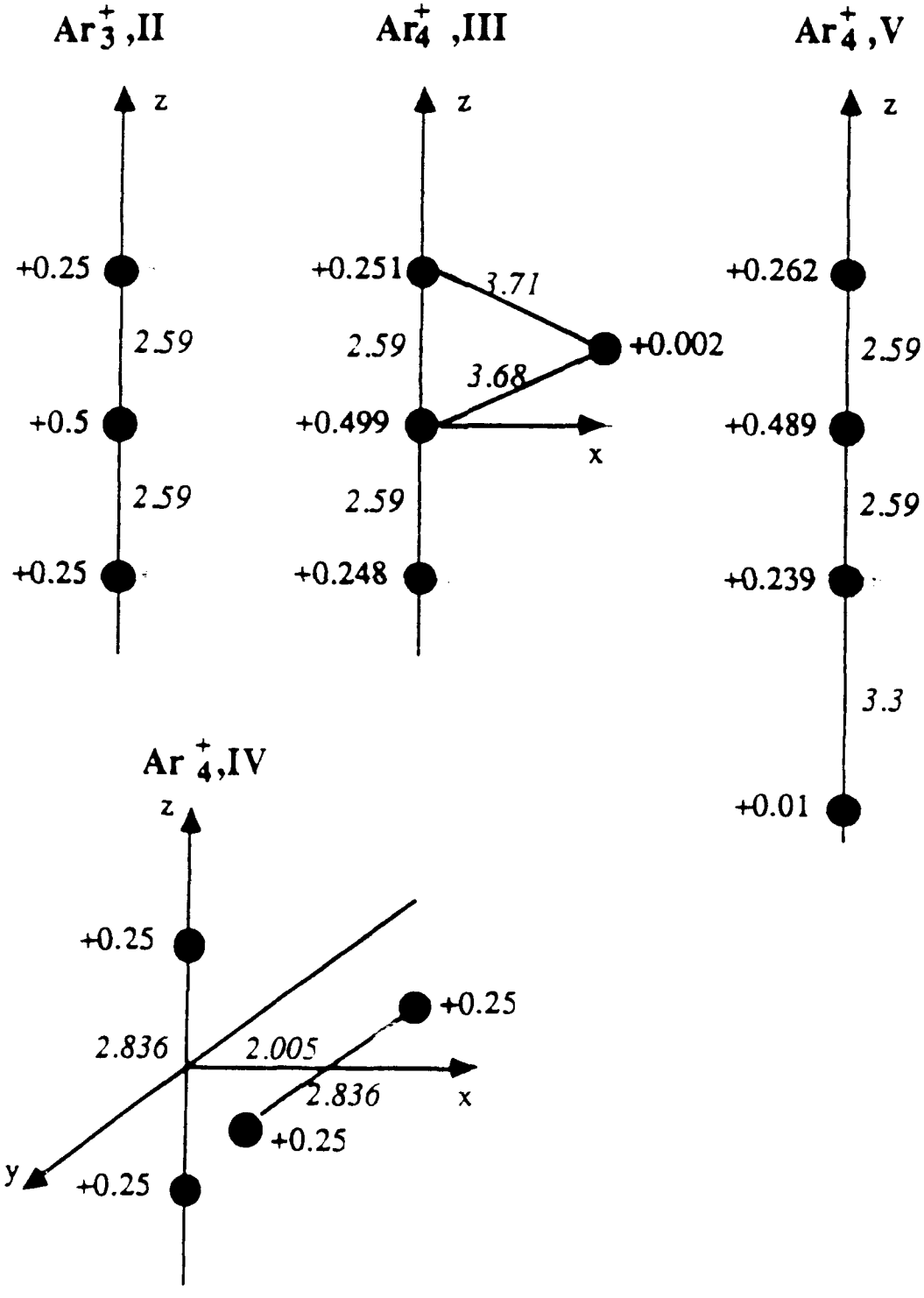
Ar_3^+,II
z
+0.25
2.59
+0.5
2.59
+0.25
Ar_4^+,III
z
+0.251
3.71
+0.002
2.59
3.68
+0.499
x
2.59
+0.248
Ar_4^+,V
z
+0.262
2.59
+0.489
2.59
+0.239
3.3
+0.01
Ar_4^+,IV
z
+0.25
+0.25
2.836
2.005
x
2.836
+0.25
y
+0.25

Figure 2

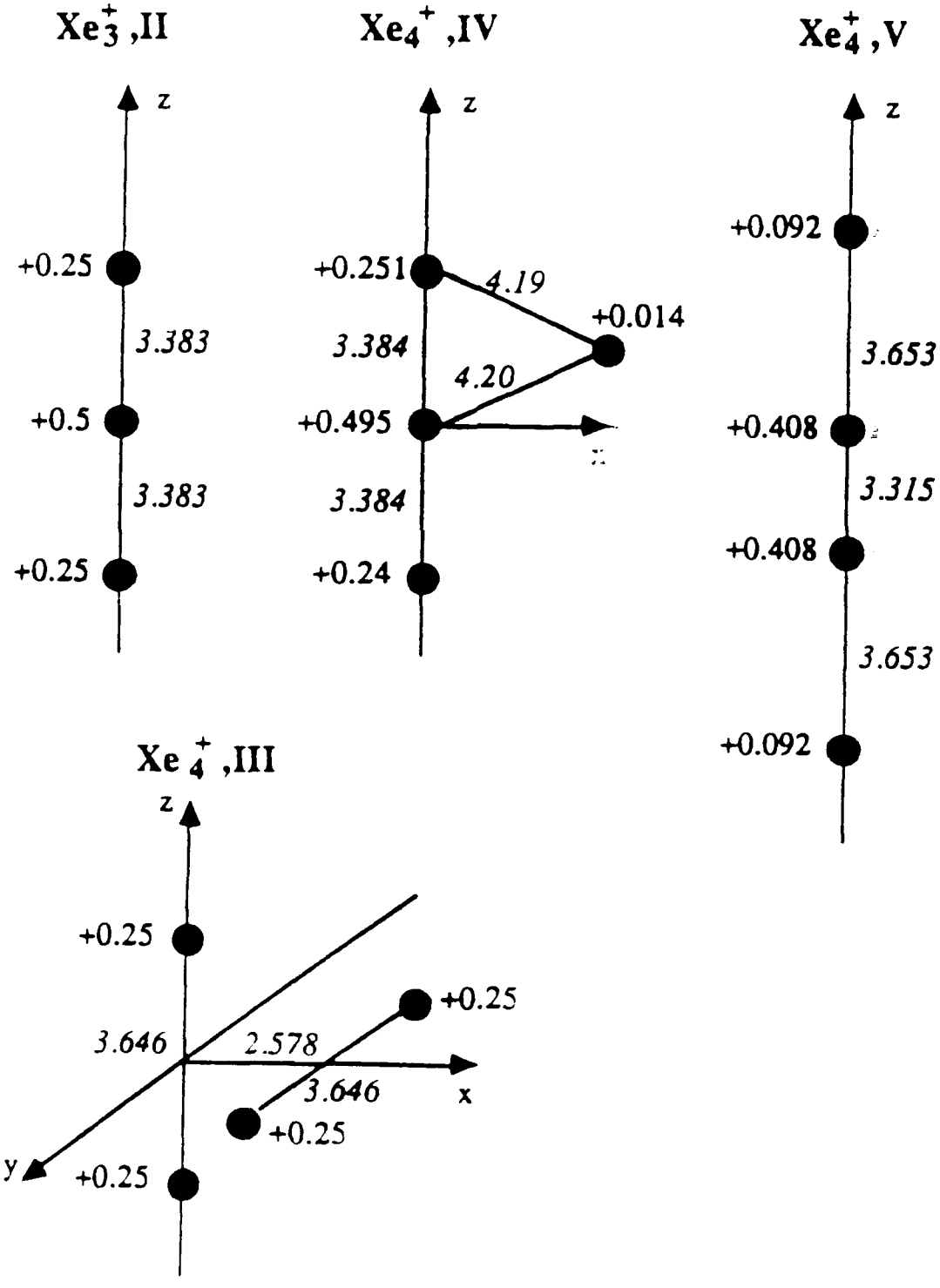
Xe_3^+ ,II
z
+0.25
3.383
+0.5
3.383
+0.25
Xe_4^+ ,IV
z
+0.251
4.19
+0.014
3.384
4.20
+0.495
x
3.384
+0.24
Xe_4^+ ,V
z
+0.092
3.653
+0.408
3.315
+0.408
3.653
+0.092
Xe_4^+ ,III
z
+0.25
+0.25
3.646
2.578
3.646
x
+0.25
y
+0.25

Figure 3

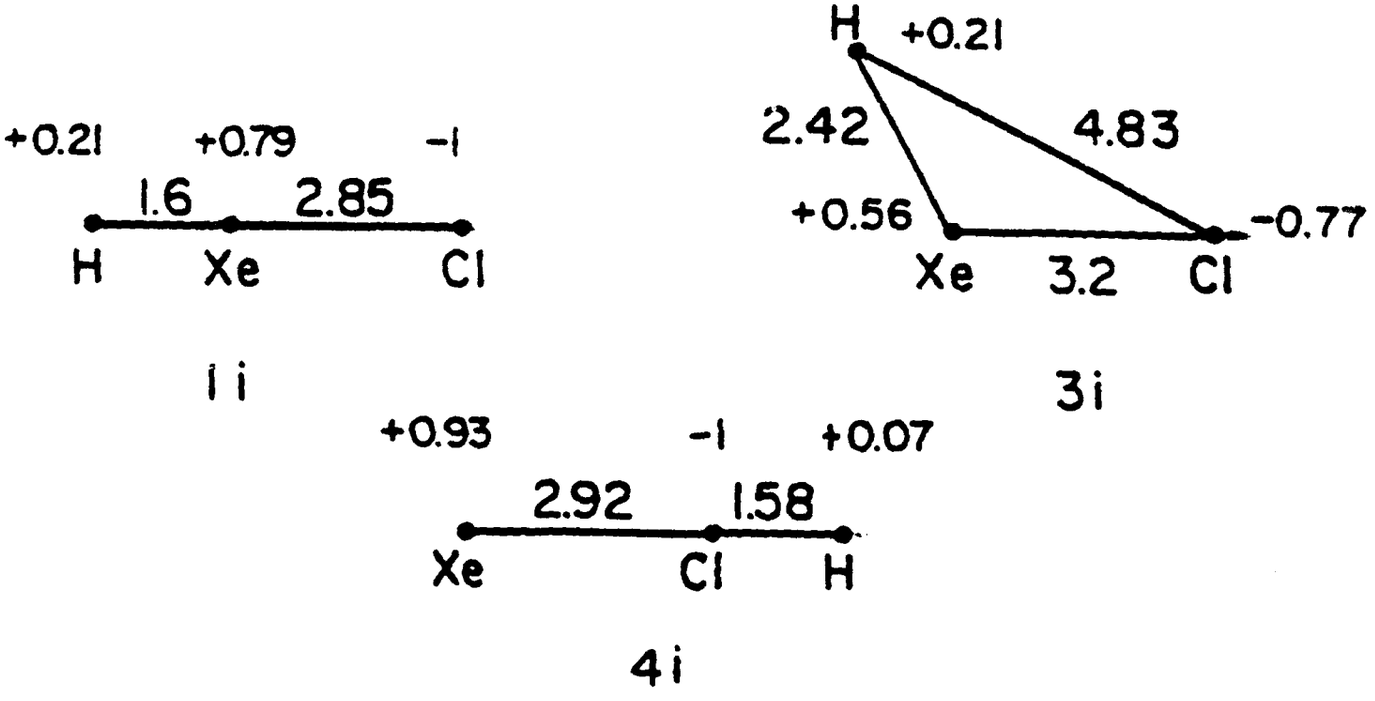

1 i

3 i

4 i

Figure 4